UNIVERSITY OF PIRAEUS

DEPARTMENT OF INTERNATIONAL AND EUROPEAN STUDIES

MASTER PROGRAM IN ENERGY: STRATEGY, LAW AND ECONOMICS

INTEGRATING ELECTRIC VEHICLES AS LOAD IN UNIT COMMITMENT

Panagiotis Adraktas

Master Thesis submitted to the Department of International and European Studies of the University of Piraeus in partial fulfillment of the requirements for the degree of Master of Science in Energy: Strategy, Law and Economics

Piraeus, May 2017

Thesis Advisor: Assistant Prof. Athanasios Dagoumas

Statutory Declaration

I, the undersigned, Panagiotis Adraktas hereby declare that this thesis has been written by myself without any external unauthorized help. Any parts, words or ideas, of this thesis, however limited, and including tables, graphs, maps etc., which are quoted from or based on other sources, have been acknowledged as such without exception. Furthermore, I hereby declare that, I am aware that in case of non-compliance with the aforementioned as certified by me, the academic title is immediately and at any time withdrawn.

ACKNOWLEDGEMENT

I would first like to thank my thesis advisor Assistant Professor Athanasios Dagoumas of the Department of International and European Studies at University of Piraeus. The door to Prof. Dagoumas' office was always open whenever I ran into a trouble spot or had a question about my research or writing. He consistently allowed this paper to be my own work, but steered me in the right direction whenever he thought I needed it.

I would also like to thank the experts who were members of the inquiry committee for this master thesis: Professor Angelos Kotios and Assistant Professor Michael Polemis.

Finally, I must express my very profound gratitude to my parents and to all my friends for providing me with unfailing support and continuous encouragement throughout my years of study and through the process of researching and writing this thesis. This accomplishment would not have been possible without them. Thank you.

Author

Panagiotis Adraktas

Integrating Electric Vehicles as Load in Unit Commitment

Keywords: unit commitment, electric vehicles, energy cost, mixed-integer linear programming, power systems

Abstract

During the last few years' electric vehicles started to catch more attention. According to environmental policies of major states and unions of states, the number of electric vehicles will be increasing in the next years. In this thesis is studied the problem of unit commitment with high penetration of renewable sources, by presenting different methods for forecasting the renewable production. Furthermore, a model of a flexible load from electric vehicles is integrated into the unit commitment models. The aim of this research is to study the impact of the excessive load on the production side and compare different unit commitment models. It is demonstrated that optimized charging is cheaper than random charging for all the models and allows higher numbers of electric vehicles to be integrated into the electric system. Simulations showed that the cost of energy increased slightly by 1% for the optimized charging profile when using 100% electric vehicles penetration, whereas in the random charging profile the increase was around 15% for the same percentage of electric vehicles penetration.

Index

Tables Index

Figures Index

Chapter 1: Introduction

1.1 Introduction

Electricity has become a necessity in the 21^{st} century in addition to that it is a valuable resource for production. Most of our modern devices such as personal computer, house electric appliances, smartphones need electric power to operate. In 2015 European Commission published a plan for the Energy Union (European Commission, 2017). The targets of the Energy Union are the security of supply, energy efficiency, reduction of greenhouse gasses emissions, enhancement of research and innovations in the Energy sector and integration of the internal market. As a result, electricity markets started playing an important role since the European Union decided that the old model of one state-owned electricity provider should be transformed into a competitive market, to achieve the targets mentioned above. Consequently, the operations of the power sector were divided into four categories.

1. Production
2. Transmission
3. Distribution
4. Supply

The generation of electricity and supply of electricity to the final users are two competitive markets. However, transmission and distribution of electricity are regulated markets. There are two key factors in order the market to perform well. The first one is the financial transparency of the Energy market; the second one is the robustness of the power system.

Thus, transmission system operators, which are responsible for the unit dispatch and solve the problem of the unit commitment, play a significant role in the whole market as they ensure the stability of the power grid and operate the cross-border interconnections, which play a major role in the Energy Union target.

In the same context of Energy Union, specifically for the decrease of the greenhouse gasses emissions European Union states encourage the installation of renewable power sources such as Photovoltaics, Wind energy plants, Biomass, small hydroelectric power plants. However, the mass installation of renewable energy sources and especially wind power plants introduce a high level of uncertainty in the unit commitment problem because their production depends on the wind speed and its stochastic nature.

The most recent addition to the target of a reduction of greenhouses gasses emissions is the electrification of the transportation sector and the in particular introduction of electric vehicles. Electric vehicles do not only help to reduce the greenhouse gasses emissions but also contribute to improve energy efficiency and enhance the innovation and research in the energy sector.

In this study, we integrate electric vehicles as load in the unit commitment problem, to investigate the quantitative impact of the extra load on the power system and the cost of energy regarding different unit commitment problems.

1.2 Outline

In Chapter 2 we present different unit commitment models. At first, we analyze the mathematical formulation of the models. Then we introduce the input data and the modification options of the implementation of these models. Finally, we present the major differences between the models.

In Chapter 3 we are studying the electric vehicles load and create a model for integration with the unit commitment models. At first, we use different statistical surveys to calculate a representative number of electric vehicles that could be introduced to our power system. Secondly, we study the current electric vehicles, to create a representative electric vehicle with certain characteristics such as battery capacity, energy efficiency. Finally, it is presented a driving pattern derived from different national authorities of European countries that could represent the habits of an average driver in the European Union. Using all those parameters, we create the model of the load coming from the use of electric vehicles.

In Chapter 4 we present the formulation of the model integrating the load from electric vehicles to a selection of unit commitment models from previous chapter 2. Then we introduce the input data from the model, along with assumptions and some simplifications on the model. Afterward, we analyze the charging profiles used for the evaluation of the impact of the load coming from the electric vehicles. Finally, we present the results of the simulations and compare the results of different models as well as the results of different charging profiles.

In Chapter 5 we make a general assessment of the research done and present the final conclusions. Moreover, suggestions for further research and improvement on the topic are made.

CHAPTER 2: Unit Commitment Problem

2.1 Introduction

The aim of a unit commitment algorithm (UC) is to determine which units will produce energy each hour of a day to meet the demand. The problem is solved in a way that the overall fuel cost is minimized in respect with the system's and unit's constraints (Simoglou, Biskas, & Bakirtzis, 2010).

The UC problem is fairly complicated. There are constraints for the elements of a power system such as the production units and the transmission lines. Each transmission line has a certain transfer capability which is called transfer capacity and suggests the maximum energy that could be transferred each hour from one side to other. The thermal production units are complicated machines, and they impose many constraints. To begin with, there is the maximum power constraint and the technical minimum which specify the range of the output of each unit. Secondly, there is the flexibility of the unit which is described by the ramp-up and ramp-down capabilities of each unit. The flexibility of a unit is the maximum rate of increase and decrease capability of output power in an hour period. More technical constraints are the start-up cost and the shut-down cost which is a considerable amount in the case of coal-fired units. Finally, we should also consider the minimum uptime and minimum downtime of a unit which is the minimum time that a unit should be committed, before shutting it down and respectively if it is shut-down, the minimum time that should be closed before starting up again.

The model that will be described and used later is based on mixed integer linear programming (MILP) which is adequate to handle such complicated problems. MILP is a method for operational research that could solve many problems; the researcher can adjust the level of optimization according to the resources and time available. The models that will be presented in this chapter were developed by the Renewables Energy Analysis Lab at the University of Washington (Renewable Energy Analysis Lab - Library, 2017).

2.2 Mathematical model

2.2.1 Nomenclature

A. Sets

B Index of generating unit cost curve segments, 1-*B*

I Index of generating units, 1-*I*

J Index of generating unit start-up cost, 1-*J*

L Index of transmission lines, 1-*L*

S Index of bus bars, 1-*S*

T Index of hours, 1-*T*

B. Parameters

a_i Fixed production cost of unit *i* ($)

B_{sm} Admittance of transmission line between nodes *s*-*m* (S)

$d_s(t)$ Load demand at bus *s* (MW)

g_i^{down} Minimum downtime of unit *i* (h)

g_i^{up} Minimum up time of unit *i* (h)

$g_i^{down,init}$ Time that unit *i* has been down before *t*=0 (h)

$g_i^{up,init}$ Time that unit *i* has been up before *t*=0 (h)

g_i^0 Output of unit *i* at *t*=0 (MW)

g_i^{max} Rated capacity of unit *i* (MW)

g_i^{min} Minimum output of unit *i* (MW)

g_{ib}^{max} Capacity of segment b of the cost curve of unit *i* (MW)

g_i^{on-off} On-off status of unit *i* at *t*=0, equal to 1 if $g_i^{up,init} > 0$, otherwise 0

k_{ib} Slope of the segment *b* of the cost curve of unit *i* ($/MW)

l_{sm}^{max} Capacity of the transmission line between nodes *s*-*m* (MW)

$L_i^{down,min}$ Length of time that unit *i* has to be off at the start of the planning horizon (h)

$L_i^{up,min}$	Length of time that unit *i* has to be on at the start of the planning horizon (h)
M	Large number used for linearization
$ramp_i^{down}$	Ramp-down limit of unit *i* (MW/h)
$ramp_i^{up}$	Ramp-up limit of unit *i* (MW/h)
suc_{ij}^{cost}	Cost steps in start-up cost curve of unit *i* ($)
suc_{ij}^{lim}	Time steps in start-up cost curve of unit *i* (h)

C. Variables

$C_i(t)$	Operating cost of unit *i* at time *t* ($)
$count_i^{down}$	Unit *i* downtime period counter
$g_i(t)$	Output power of unit *i* at time *t* (MW)
$g_{ib}(t)$	Output power of unit *i* on segment b at time *t* (MW)
$suc_i(t)$	Start-up cost of unit *i* at time *t* ($)
$w_{ij}(t)$	Binary variable equal to 1 if unit *i* is started at time *t* after being out for *j* hours, otherwise 0
$x_i(t)$	Binary variable equal to 1 if unit *i* is producing at time *t*, otherwise 0
$y_i(t)$	Binary variable equal to 1 if unit *i* is started at the beginning of time *t*, otherwise 0
$z_i(t)$	Binary variable equal to 1 if unit *i* is shutdown at the beginning of time *t*, otherwise 0
$\theta_s(t)$	Voltage angle at bus *s* (rad)

2.2.2 Formulations

The aim is to minimize the total generation cost of the thermal power plants which is described in the following objective function (Pandžić, Qiu, & Kirschen, 2013).

$$\sum_{t=1}^{T}\sum_{i=1}^{I} C_i(t) \qquad (1)$$

Expressions (2) and (3) describe the binary logic. Specifically, expression (3) prohibits a unit starting up to be simultaneously shut down. Expression (2) implements the logic that if a unit is starting up at time t, it cannot be on at time t-1.

$$y_i(t) - z_i(t) = x_i(t) - x_i(t-1) \quad \forall\, 1 \le t \le T, i \le I \qquad (2)$$

$$y_i(t) + z_i(t) \le 1 \quad \forall\, t \le T, i \le I \qquad (3)$$

Equation (4) defines the total cost for each unit i. The total cost is the summation of the startup cost of the units (if needed), the fixed cost and the variable cost:

$$C_i(t) = \alpha \cdot x_i(t) + \sum_{b=1}^{B} k_b \cdot g_{i,b}(t) + suc_i(t) \quad \forall\, t \le T, i \le I \qquad (4)$$

The total unit output is equal to the sum of the generation in each segment of the cost curve:

$$g_i(t) = \sum_{b=1}^{B} g_{i,b}(t) \quad \forall\, t \le T, i \le I \qquad (5)$$

Minimum unit output must be higher than the minimum output of unit i:

$$g_i(t) \ge g_i^{min} \cdot x_i(t) \quad \forall\, t \le T, i \le I \qquad (6)$$

Unit output for each generation level.

$$g_{i,b}(t) \le g_{i,b}^{max} \cdot x_i(t) \quad \forall\, t \le T, i \le I, b \le B \qquad (7)$$

Minimum up time constraints:

$$\sum_{t=1}^{L_i^{up,min}} \left(1 - x_i(t)\right) = 0 \quad \forall\, i \le I \qquad (8)$$

$$\sum_{tt=t}^{t+g_i^{up}-1} x_i(tt) \ge g_i^{up} \cdot y_i(t) \quad \forall\, L_i^{up,min} + 1 \le t \le T - g_i^{up} + 1, i \le I \qquad (9)$$

$$\sum_{tt=t}^{T}\left(x_i(tt)-y_i(t)\right) \geq 0 \quad \forall\, T-g_i^{up}+2 \leq t \leq T, i \leq I \qquad (10)$$

where $L_i^{up,min} = max\left\{0, min\left\{T, \left(g_i^{up} - g_i^{up,init}\right) \cdot g_i^{on-off}\right\}\right\}$

Minimum down time constraints:

$$\sum_{t=1}^{L_i^{down,min}} x_i(t) = 0 \quad \forall\, i \leq I \qquad (11)$$

$$\sum_{tt=t}^{t+g_i^{down}-1} \left(1-x_i(tt)\right) \geq g_i^{down} \cdot z_i(t) \quad \forall\, L_i^{down,min}+1 \leq t \leq T-g_i^{down}+1, i \leq I \qquad (12)$$

$$\textstyle\sum_{tt=t}^{T}\left(1-x_i(tt)-z_i(t)\right) \geq 0 \quad \forall\, T-g_i^{down}+2 \leq t \leq T, i \leq I \qquad (13)$$

where $L_i^{down,min} = max\left\{0, min\left\{T, \left(g_i^{down} - g_i^{down,init}\right) \cdot \left(1-g_i^{on-off}\right)\right\}\right\}$

Ramp-up and ramp-down constraints:

$$-ramp_i^{down} \leq g_i(t) - g_i(t-1) \quad \forall\, 2 \leq t \leq T, i \leq I \qquad (14)$$

$$ramp_i^{up} \geq g_i(t) - g_i(t-1) \quad \forall\, 2 \leq t \leq T, i \leq I \qquad (15)$$

$$-ramp_i^{down} \leq g_i(t_1) - g_i^0 \quad \forall\, i \leq I \qquad (16)$$

$$ramp_i^{up} \geq g_i(t_1) - g_i^0 \quad \forall\, i \leq I \qquad (17)$$

Expression (18) and equations (19) and (20) impose the constraints and calculate the startup cost of each unit i. Specifically, inequation (18) sets the limitations for the calculation of the value of variable $w_{ij}(t)$, taking into account the initial conditions.

$$w_{ij}(t) \leq \sum_{tt=suc_{ij}^{lim}}^{min\left\{t-1, suc_{i,j+1}^{lim}-1\right\}} z_i(t-j) + 1\$\left\{j \leq J-1 \land suc_{i,j}^{lim} \leq g_i^{down,init}+t-1 < suc_{i,j+1}^{lim}\right\} + 1\$\left\{j = J \land suc_{i,j}^{lim} \leq g_i^{down,init}+t-1\right\} \quad \forall\, t \leq T, i \leq I, j \leq J \qquad (18)$$

$$\sum_{j=1}^{J} w_{ij}(t) = y_i(t) \quad \forall\, t \leq T, i \leq I \qquad (19)$$

$$suc_i(t) = \sum_{j=1}^{J} suc_{ij}^{cost} \cdot w_{ij}(t) \;\; \forall\, t \leq T, i \leq I \qquad (20)$$

Where symbol $ represents logical IF and symbol ∧ symbolizes logical AND.

Equation (21) defines the power balance in the electrical system.

$$\sum_{i=1}^{I} g_i(t) - \sum_{\{s,m\}\in L|m>s} B_{sm} \cdot \left(\theta_s(t) - \theta_m(t)\right) - \sum_{\{s,m\}\in L|m<s} B_{sm} \cdot \left(\theta_m(t) - \theta_s(t)\right) \;\forall\, t \leq T, \quad s \leq S \qquad (21)$$

Transmission constraints:

$$-l_{sm}^{max} \leq B_{sm} \cdot \left(\theta_s(t) - \theta_m(t)\right) \leq l_{sm}^{max} \;\; \forall t \leq T, \{s,m\} \in L \qquad (22)$$

$$-\pi \leq \theta_s(t) \leq \pi \;\; \forall t \leq T, s \leq S \qquad (23)$$

$$\theta_s(t) = 0 \;\; \forall t \leq T \qquad (24)$$

2.3 Implementation

Based on the previously described formulation REAL developed five different implementations of the Unit Commitment problem. The application of the model is on a power system based on IEEE RTS-96. This power system includes, apart from thermal production units of various fuel (nuclear, coal-fired, diesel, natural gas), renewable energy generation units from the wind. Specifically, there are 19 wind power plants of total wind production capacity of 6900MW. The wind power plants are distributed in the following way: 3900 MW in the West subsystem, 2400 MW in the central subsystem and 600 MW in the east subsystem. There are also 73 buses, 120 transmission lines, 96 thermal power units and 51 loads. The whole system can be seen in the following layout.

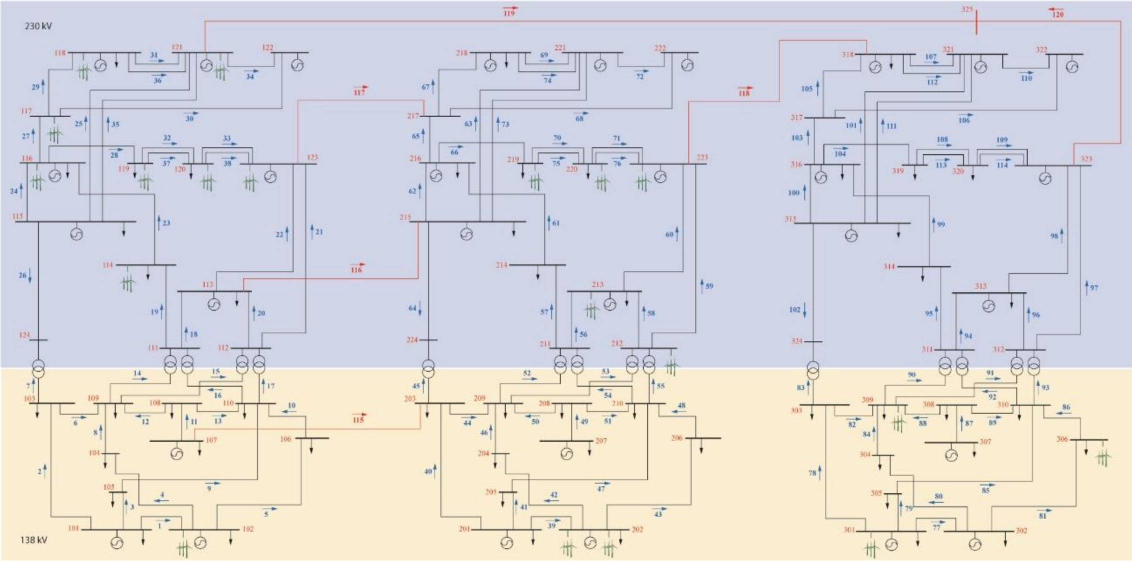

Figure 1-The electrical system IEEE RTS-96

The inclusion of renewable energy sources in a power system introduces uncertainty on the real production of those units. The uncertainty comes from the stochastic nature of the wind and the weather conditions in general. Transmission system operators have to forecast the real output from those renewable sources to calculate the thermal power needed to meet the electricity demand and ensure the system stability. The stochastic wind power production is a major parameter in the system instability, and the high penetration of renewable production must be compensated with the installation of flexible thermal production units or hydropower, which can increase and decrease their output rapidly. As a matter of fact, the forecasting of the renewable energy sources real output is a major problem for the transmission system operators. It affects the stability of the power system and the energy market participants as well as the energy markets itself.

The models that we will present are the following:

- Deterministic unit commitment
- Stochastic unit commitment
- Improved interval unit commitment
- Interval unit commitment
- Robust unit commitment

Each of those models uses a different mathematical procedure to forecast the anticipated renewable production. Some of them are more preservative than the others. Consequently, it is committing more thermal units, and the stability of the system is increased but with a higher economic cost.

2.3.1 Input Data

All five models use the same excel file as data input file. That file includes all the tables needed for the calculations. GAMS read the input data through a small program, which provides the users the options to change some parameters before running the unit commitment model. In the following paragraph, we present briefly the options available and the data loaded from the Data input code (Renewable Energy Analysis Lab - Library, 2017).

Options

At first, we have the option to change some constants in the Data input program. Through those options, we can modify the penetration of the renewable sources, the variable cost, and ramping capabilities of thermal units, the capacities of the transmission lines, the wind profile and a penalty factor in the case of spilled wind production or unserved loads. In our research, we choose to have 30% of energy from renewable sources, which is much higher than the current state of most power grids. Another decision is to go with the unfavorable wind profile. In the following figure, we can see the graph of the load and the unfavorable wind profile.

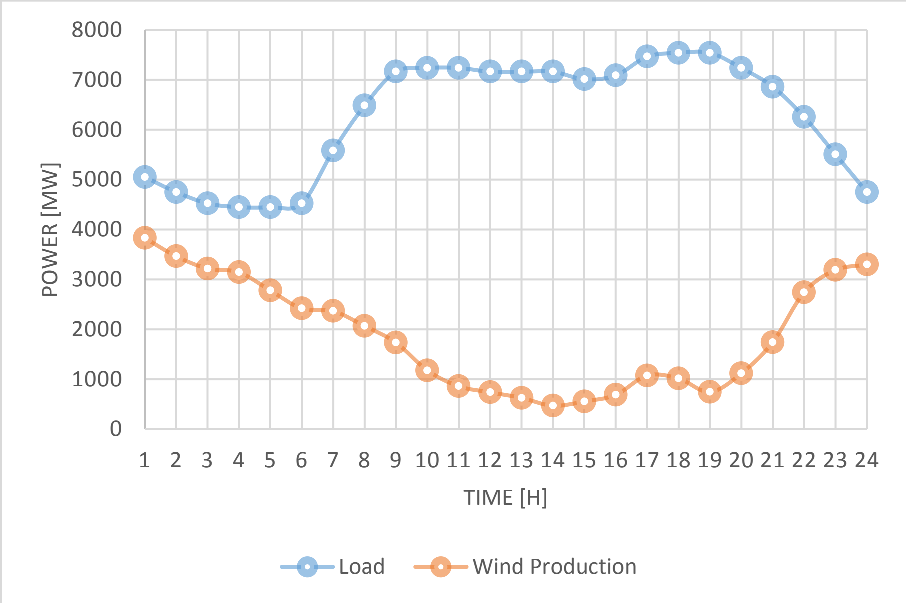

Figure 2-Load profile and wind production profile.

The favorability of the wind profile is defined by the load curve. If both curves increase and decrease simultaneously, then we have a favorable wind profile. In our research, we want to stress the algorithm and test its results in non-favorable situations. Therefore, we chose the unfavorable wind profile shown above.

Parameters

In the following tables is shown the form of the input data as they are inserted into the model.

Thermal unit data

Table 1-Units map gen_map(i,s): includes the position of each unit in the power system.

	s101	**s102**	**s103**	**s104**	**s105**
i1	1	0	0	0	0
i2	1	0	0	0	0
i3	1	0	0	0	0

Table 2-The capacity of segment b of the cost curve of unit i (MW): g_max(i,b).

Output Block (MW):

	b1	b2	b3
i1	6,666667	6,666667	6,666667
i2	6,666667	6,666667	6,666667
i3	25,33333	25,33333	25,33333

Table 3-The slope of segment b of the cost curve for unit i ($/MW): k(i,b).

Cost ($/MW):			
			tr4
i1	**.**	**b1**	28,967
i1	**.**	**b2**	29,243
i1	**.**	**b3**	29,703
i2	**.**	**b1**	28,957
i2	**.**	**b2**	29,233
i2	**.**	**b3**	29,693

Table 4-Cost steps in start-up cost curve of unit i ($) suc_sw(i,j)

Start-up Cost ($):			
			tr4
i1	**.**	**j1**	25
i1	**.**	**j2**	28
i1	**.**	**j3**	31
i1	**.**	**j4**	34
i1	**.**	**j5**	37
i1	**.**	**j6**	40

i1	**.**	**j7**	43
i1	**.**	**j8**	46
i2	**.**	**j1**	25
i2	**.**	**j2**	28
i2	**.**	**j3**	31
i2	**.**	**j4**	34
i2	**.**	**j5**	37
i2	**.**	**j6**	40
i2	**.**	**j7**	43
i2	**.**	**j8**	46

Table 5-Time steps on start-up cost curve of unit i (h) suc_sl(i,j)

Start-up Blocks (h):								
	j1	**j2**	**j3**	**j4**	**j5**	**j6**	**j7**	**j8**
i1	1	2	3	4	5	6	7	8
i2	1	2	3	4	5	6	7	8
i3	1	2	3	4	5	6	7	8

Table 6-Time periods that unit i has been down before t=0 (h): count_off_init(i)

Count "off" Init (h)	
	column1
i1	0
i2	0
i3	0

i4	1
i5	17
i6	4

Table 7-Time that unit i has been up before t=0 (h): count_on_init(i)

Count "on" Init (h)	
	column1
i1	1
i2	400
i3	220
i4	0

Table 8-Fixed production cost for unit i ($): a(i)

No Load Cost ($)	
	tr4
i1	454,572
i2	454,562
i3	263,419

Table 9-Ramp up limit of unit i (MW/h): ramp_up(i)

Ramp Up Limit (MW/h)	
	tr4

i1	30,5
i2	30,5
i3	38,5

Table 10-Ramp down limit of unit i (MW/h): ramp_down(i)

Ramp Down Limit (MW/h)	
	tr4
i1	70
i2	70
i3	80

Table 11-Minimum time a unit i has to be shut down (h): g_down(i)

Min. Down Time (h)	
	tr4
i1	1
i2	1
i3	2

Table 12-Minimum time a unit i has to be up (h): g_up(i)

Min. Up Time (h)	
	tr4
i1	1

i2	1
i3	3

Table 13-Minimum output capacity of unit i (MW): g_min(i)

Min. Output (MW)	
	tr4
i1	4
i2	4
i3	15,2

Table 14-Output power of unit i at time periodt=0 (MW): g_0(i)

Output at t=0 (MW)	
	column1
i1	20
i2	20
i3	70
i4	0
i5	0

Transmission line data

Table 15-Admittance of transmission line between nodes s-m (S): admittance(l)

1/X	
	column1

l1	7142,857
l2	473,9336
l3	1176,471

Table 16-Line map, line_map(l,s)

	s101	**s102**	**s103**	**s104**	**s105**
l1	1	-1	0	0	0
l2	1	0	-1	0	0
l3	1	0	0	0	-1
l4	0	1	0	-1	0

Table 17-Capacity of transmission line between nodes s-m (MW): l_max(l)

Capacity	
	column1
l1	175
l2	175
l3	175
l4	175

Demand load data

Table 18-Demand load on bus s (MW): d(t,s)

	s101	**s102**	**s103**	**s104**
t1	63,98618	57,25079	106,0823	43,78002
t2	60,16611	53,83283	99,74907	41,16628
t3	57,30105	51,26936	94,99911	39,20598

Wind plants data

Table 19-Wind plants map w_map(w,s)

	s116	**s117**	**s118**	**s119**
w3	1			
w4		1		
w5			1	
w6				1
w7				

Table 20-Capacity of wind plants (MW): w_capacity(w)

	column1
w1	300
w2	300
w3	600
w4	600

Table 21-Probabilities for each of the wind scenarios: prob(scen)

	column1
scen1	0,02
scen2	0,16
scen3	0,107273
scen4	0,241818
scen5	0,107273
scen6	0,15

scen7	0,086364
scen8	0,000909
scen9	0,125455
scen10	0,000909

Earlier we mentioned that we have the option to select between a favorable and an unfavorable wind profile. The input data program selects each time the appropriate table according to our selection. The procedure is the same for both wind patterns.

Table 22-w_det_pu_1(t,w): includes the available wind power for each unit i calculated in per unit values.

FAVOURABLE						
Deterministic						
Capacity	300	300	600	600	300	600
	w1	**w2**	**w3**	**w4**	**w5**	**w6**
t1	0,08638	0,211012	0,153027	0,154525	0,026973	0,48574
t2	0,043697	0,139327	0,139853	0,131191	0,076886	0,431102
t3	0,089033	0,151854	0,15494	0,179127	0,095984	0,370302
t4	0,30466	0,299134	0,273481	0,249978	0,064053	0,176555
t5	0,396127	0,299414	0,343453	0,178707	0,025651	0,066776

Table 23-Lower and upper bound of wind production: wind_robust_pu_1(t,w,robust) per unit values.

BOUNDS				
			UP	**DOWN**

			col1	col2
t1	**.**	**w1**	0,236872	0
t1	**.**	**w2**	0,337008	0,109605
t1	**.**	**w3**	0,278299	0,042769
t1	**.**	**w4**	0,271115	0,030279
t1	**.**	**w5**	0,084981	0
t1	**.**	**w6**	0,749222	0,254945

Table 24-Stochastic ramp-up and ramp-down rates of wind production: w_stoch_max_1(t,w,robust).

STOCHASTIC RAMPS				
			UP	**DOWN**
			col1	**col2**
t2	**.**	**w1**	0	-0,08988
t2	**.**	**w2**	-0,01223	-0,06527
t2	**.**	**w3**	0,121853	-0,11767
t2	**.**	**w4**	0,001779	-0,10418
t2	**.**	**w5**	0,131416	0,003539
t2	**.**	**w6**	-0,03241	-0,31289
t2	**.**	**w7**	0,010194	-0,0251
t2	**.**	**w8**	0,033926	0,000792

Table 25-Probability for each scenario for each wind unit: wind_scenarios_1(t,w,scen).

		scen1	scen2	scen3	scen4	scen5	scen6	scen7
t1	**w1**	0,100862	0,072062	0,099023	0,080163	0,132368	0,061889	0,127721

t1	**w2**	0,181467	0,220213	0,187513	0,240498	0,191013	0,170966	0,213342
t1	**w3**	0,158785	0,121393	0,160644	0,144837	0,201459	0,12883	0,161325
t1	**w4**	0,169363	0,133267	0,17627	0,116373	0,163892	0,071113	0,171963
t1	**w5**	0,021053	0	0,027147	0	0,010517	0	0,013856
t1	**w6**	0,488406	0,502584	0,442172	0,504939	0,48416	0,54788	0,481501
t1	**w7**	0,546199	0,593101	0,51642	0,61542	0,505618	0,549848	0,505922

2.3.2 Differences between the models

Deterministic Unit Commitment Model (DUC)

This model uses only one forecast for the wind production. That forecast has come out as the most probable to happen from a big amount of historical data. The solution can be either conservative or very inefficient in certain conditions because it is not calculated the probability of very low wind energy production. Thus, in high penetration levels of renewable power sources when the uncertainty is high, the credibility of such models will be low.

“power_balance(t,s)..sum(i$(gen_map(i,s)),g(t,i)) + sum(w$(w_map(w,s)),w_det(t,w)-curt(t,w))-sum(l$(line_map(l,s) <> 0),pf(t,l)*line_map(l,s)) =e= d(t,s)”

Where the second element of the formula represents the finally used wind energy production.

Stochastic Unit Commitment Model (SUC)

The stochastic model uses a different approach in the calculation of the wind production. Instead of using a fixed forecast it calculated the unit commitment for ten different wind scenarios and then weights the solution with the probabilities for each scenario.

The power balance formula for this model is:

“power_balance(t,scen,s)..sum(i$(gen_map(i,s)),g(t,scen,i))+sum(w$(w_map(w,s)),wind_scenarios(t,w,scen)-curt(t,scen,w))-sum(l$(line_map(l,s)<>0),pf(t,scen,l)*line_map(l,s)) =e= d(t,s)”

The model produces one solution for all the scenarios (10). As a result, there might be a situation where a scenario may be closer to the reality, however, the probability of this scenario is very low. Then the final solution will not be so close to that scenario but will be optimized for all the scenarios and not separately for each one of them. Consequently, the total cost will be higher than in the deterministic model solution. It is possible though, to reduce that effect by rejecting loads or spilling wind production in certain cases. In the event of an extreme scenario, the system operator might decide that it is better to shed a load instead of committing a very expensive thermal unit. Each transmission system operator decides whether this is an option or not according to the valuation of the spilled RES production and the unserved loads. The solution produced by SUC carries a certain amount of unhedged uncertainty. This uncertainty is quantified regarding expected unserved loads and spilled production (Dvorkin, Pandžić, Ortega-Vazquez, & Kirschen, 2015).

Interval Unit Commitment Model (IUC)

In this model, we have a simplified representation of the uncertainty coming from the renewable sources production. We use as a central scenario the deterministic scenario we utilized for the deterministic model. Additionally, we have an upper bound scenario for the wind energy production and a lower bound scenario.

The following code implements those scenarios:

```
“*BEST GUESS

g_wind(t,w,'u1')=w_det(t,w);

*UPPER LIMIT

g_wind(t,w,'u2')=wind_robust(t,w,'col1');

*LOWER LIMIT

g_wind(t,w,'u3')=wind_robust(t,w,'col2');”
```

The model minimizes the objective function over the deterministic wind forecast. Furthermore, we use upper and lower bound forecasts to create extreme situations for the ramp up and ramp down limits for the thermal units.

The following code lines implement that logic:

“ramp_det_dn(t,u,i)$(ord(t) lt card(t)).. g(t,'u1',i) - g(t+1,'u3',i) =l= ramp_down(i);

ramp_det_up(t,u,i)$(ord(t) lt card(t)).. -g(t,'u1',i) + g(t+1,'u2',i) =l= ramp_up(i);

ramp_lower_up(t,i)$(ord(t) lt card(t)).. -g(t,'u3',i) + g(t+1,'u2',i) =l= ramp_up(i);

ramp_upper_dn(t,u,i)$(ord(t) lt card(t)).. g(t,'u2',i) - g(t+1,'u3',i) =l= ramp_down(i);”

This way we secure that there is a solution for every scenario between the upper and lower bounds we used to create the ramp up and ramp down cases. The produced solution is more expensive than the solution of SUC because it foresees extreme load transitions for the ramp-up and ramp-down limits. In reality, those scenarios although they might be possible the probability of happening is very low, and the model does not take into account that aspect. The increased reliability is ensured by committing more units. Consequently, that increases the economic cost of the solution. In contrary with SUC model, there is no unhedged uncertainty in IUC model since all the possible scenarios are within those, which were used for the calculation of the upper and lower bounds. The following figure describes the model graphically (Pandzic, Dvorkin, Wang, Qiu, & Kirschen, 2016).

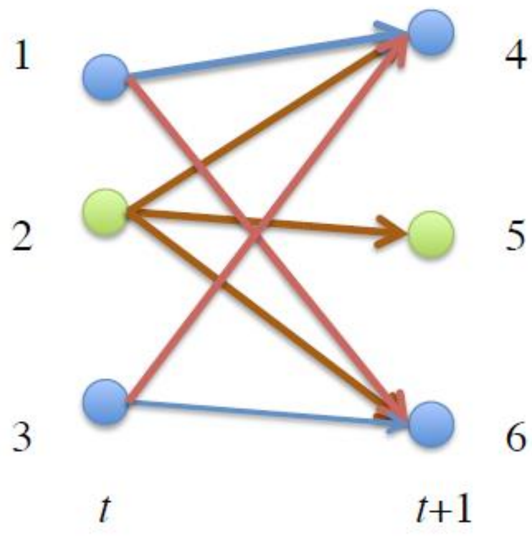

Figure 3-Ramp-up and ramp-down transitions for the interval unit model (Kirschen, Pandzic, Dvorkin, Wang, & Qiu, 2017).

Improved Interval Unit Commitment Model (IIUC)

Improved Interval Unit Commitment Model (IIUC) is an enhanced version of the previous model (IUC). Instead of two scenarios (upper and lower bound of wind production), we have four scenarios. To create the two additional scenarios, we introduce a new set of data with the higher wind production transitions between the scenarios (increasing and decreasing). The central scenario remains the same as in the previous models, however, now there are two scenarios for the ramp up and two for the ramp down limits.

The following code lines implement the previous logic:

```
"*BEST GUESS

g_wind(t,w,'u1')=w_det(t,w);

*UP RAMPING ODD

g_wind(t,w,'u2')=wind_robust(t,w,'col1')$(mod(ord(t),2)=1)+(wind_robust(t+1,w,'col1')
-(wind_stoch_max(t+1,w,'col1')))$(mod(ord(t),2) = 0);

*UP RAMPING EVEN
```

g_wind(t,w,'u3')=wind_robust(t,w,'col1')$(mod(ord(t),2)=0)+(wind_robust(t+1,w,'col1') -(wind_stoch_max(t+1,w,'col1')))$(mod(ord(t),2) = 1);

*DOWN RAMPING ODD

g_wind(t,w,'u4')=wind_robust(t,w,'col2')$(mod(ord(t),2)=1)+(wind_robust(t+1,w,'col2') -(wind_stoch_max(t+1,w,'col2')))$(mod(ord(t),2) = 0);

*DOWN RAMPING EVEN

g_wind(t,w,'u5')=wind_robust(t,w,'col2')$(mod(ord(t),2)=0)+(wind_robust(t+1,w,'col2') -(wind_stoch_max(t+1,w,'col2')))$(mod(ord(t),2) = 1);"

In IIUC model, we use the same limits as in the IUC. We use scenarios u2 and u4 for the ramp-up and ramp-down boundaries of odd time periods and u3, u5 for even time periods accordingly. The following example explains how this model calculates the ramp up and ramp down limits. Let's say that we have an upper bound for wind production in period t=2 at 50MW and the highest slope among our wind scenarios is 20MW/h then the particular scenario for period t=1 will start from 30MW and end at 50 MW at period t=2. The following code lines implement this logic:

"ramp_limit_min(t,u,i)$(ord(t) gt 1 and (ord(u)=1 or(ord(u)=4 and (mod(ord(t),2) = 1)) or (ord(u)=5 and (mod(ord(t),2) = 0))))-ramp_down(i) =l= g(t,u,i) - g(t-1,u,i);

ramp_limit_max(t,u,i)$(ord(t) gt 1 and (ord(u)=1 or(ord(u)=2 and (mod(ord(t),2) = 1)) or (ord(u)=3 and (mod(ord(t),2) = 0))))ramp_up(i) =g= g(t,u,i) - g(t-1,u,i);"

This model uses the same logic as the previous one but with modified extreme transition cases. Now the thermal production has to cope with reduced transition slopes. Instead of using transitions from the lowest bound to the highest now we use more realistic slopes by using the same upper and lower bounds but also including the highest ramp-up and ramp-down from the wind scenarios. This approach is much more realistic because the previous extreme transition values are not possible to happen in real world. As a result, we anticipate IIUC solution to be less expensive than IUC. The following figure shows a graphic representation of the logic described before (Pandzic, Dvorkin, Wang, Qiu, & Kirschen, 2016).

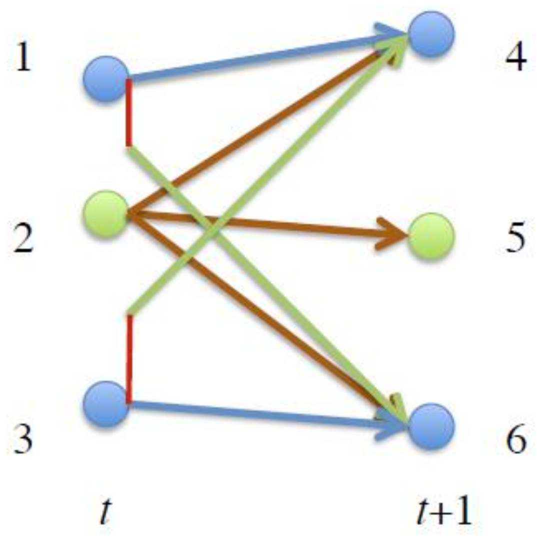

Figure 4-Ramp-up and ramp-down transitions for the improved interval unit model (Kirschen, Pandzic, Dvorkin, Wang, & Qiu, 2017).

Robust Unit Commitment Model

The objective function of the model is the following (Bertsimas, Litvinov, Sun, Zhao, & Zheng, 2013):

$$\sum_{t=1}^{T}\sum_{i=1}^{I}\left(\alpha \cdot x_i(t) + suc_i(t)\right) + max\left\{\sum_{b=1}^{B} k_b \cdot g_{i,b}(t)\right\} \quad \forall\, t \leq T, i \leq I \qquad (25)$$

The first two elements of the expression represent the startup cost and fixed production cost of the units. The third element represents the variable production cost in the worst-case scenario, which is the difference between all the previous models. The optimization is made on the worst scenario instead of best guessed (deterministic) scenario. For this reason, it is considered as a conservative unit commitment model with increased robustness.

The solution of the problem is divided into two stages (Bertsimas, Litvinov, Sun, Zhao, & Zheng, 2013). In the first stage, it decides which units will be committed by taking into account the fixed costs and the start-up costs. Once it is decided which units will be dispatched, then it is calculated the output power of the units respecting the reserves that will be needed in the worst-case scenario.

The level of uncertainty in this model is quantified in the number of wind plants that their real production can deviate from the forecast. If we select all the wind plants, then it will solve the most conservative scenario. On the other hand, if we select none plants it will solve the deterministic scenario.

2.4 Conclusion

According to the theoretical model differences (Kirschen, GridOPTICS, 2017) confirms those results. The following figure summarizes the differences between the different models. The difference is more evident in the unfavorable wind profile than in the favorable wind profile.

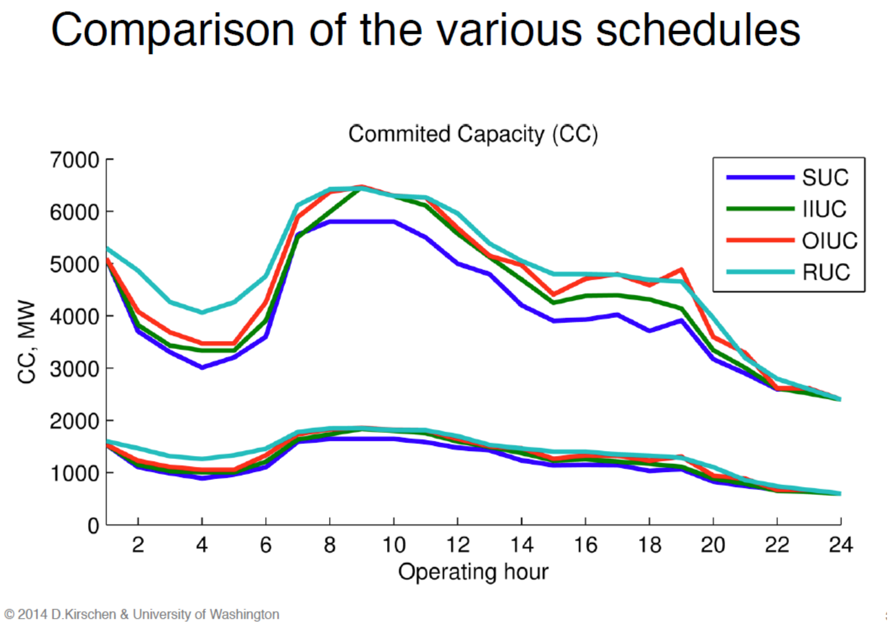

Figure 5-Committed capacity (Kirschen, GridOPTICS, 2017).

Chapter 3: Electric Vehicles and Driving pattern

3.1 Introduction

During the last years, electrification of mobility is a matter of crucial importance in the US, Japan, China and EU. Especially in the EU it is an issue that falls within the 20-20-20 energy and climate target (Europe 2020 in a nutshell, 2017) and the long-term ambition for drastic decarbonization by 2050 (European Environment Agency, 2017). The 20-20-20 package has led to the definition of targets such as the reduction of greenhouse gas emissions, the increase of renewable sources share in final energy consumption and the improvement of energy efficiency (European, Parliament, & Counsil, 2009). The electricity sector together with the transportation sector produce nearly two-thirds of global CO2 emissions, and almost 75% of those comes from road transports. Furthermore, apart from the environmental problems caused by using fossil fuels for transport and electricity production we should also take into account the depletion of those finite energy sources and the dependence on them. In the EU, a percentage of 73% of all oil is consumed by the transport sector (C6.20, 2015). In addition to that EU is not a producer but an importer of fossil fuels, a reality which might further create economic and geopolitical concerns.

The introduction of a vast number of electric vehicles in modern power systems will affect a wide variety of factors in the operation of power systems and markets of electricity. First of all, the power systems and the distribution networks will be loaded with extra power during the peak hours (GRAHN, 2013). That will create the need for additional power production capacity available, as well as for more capacity available both for the transfer and the distribution networks (Clement-Nyns, Haesen, & Driesen, 2009). Another crucial factor is the stability of the system which will be highly affected by both the stochastic production of the renewable sources and the stochastic charging of the electric vehicles. Finally, the prices of electricity will be affected, depending on the ways that will be decided to produce the extra energy that will cover the electrified mobility demand (Schill & Gerbaulet, 2015). Last but not least, we should consider the impact of the additional power generation on the environment. Studies have indicated that if the electricity is produced by "dirty" power plants, then the reduction of gas emissions is negligible, making thus the electrification of road transports an ineffective measure for gas emissions reduction (Kasten, Bracker, Haller, & Purwanto, 2016).

The effects that were previously discussed might be deterrent for the adoption of electric vehicles in large scale. On the other hand, all these effects create opportunities for the smarter approach of the operation of all those sectors. To begin with, we should consider that a greater penetration of renewable sources combined with electric vehicles will lead to a reduction of gas emissions from the transport sector (Willett & Jasna, 2005). Secondly, the investments on production capacity and transfer/distribution capacity could be reduced with the introduction of smart charging technologies and Vehicle to Grid services. Thirdly, big parking lots could be used as Load aggregators who could provide ancillary services for the systems during peak hours, something that could further lead to a reduction in the usage cost for the vehicle owner (Boumis, 2012).

The research carried out in this chapter regards the effect of extra load coming from electric vehicles' charging to the electric system which was discussed in chapter 2. Specifically, we use three different charging profiles. Profile 1 leaves the decision to the unit commitment algorithm to choose the best hours for the extra load. Profile 2 simulates the charging of electric vehicles right after their trips. Profile 3 simulates the charging only during off-peak hours 1-8 and 21-24. We mainly focus on the effects on the average energy price, depending on the percentage of electric vehicles penetration and the effects on the system load under different charging profiles.

The research was carried out using the system and algorithms described in the previous chapter, following the addition of a small model on driving patterns and electric vehicles characteristics which lead to an additional load demand.

3.2 Electric Vehicles

3.2.1 Number of electric vehicles

In western countries, such as the US, Germany, Japan, France, Italy, the yearly electricity production per capita ranges between 5000kWh/cap to 12000kWh/cap (The World Factbook, 2017). Thus, we derive that an average of about 8500kWh/cap will be used for our calculations, which means that we have an average of 1kW/cap of annual power level.

The power system that we used in the previous chapter consisted of 10215MW of thermal energy production capacity, according to our previous calculations that mean that this power system is the equivalent system for a population of 10,215 million people.

Table 26-Consumption of electricity

Country	Population	Electricity Consumption (kWh)	Electricity Consumption/cap(kWh)
EU	513949445	2,771E+12	5446
USA	323995528	3,913E+12	12199
Japan	126702133	9,34E+11	7446
Germany	80722792	5,33E+11	6669
France	66836154	4,31E+11	6513
UK	64430428	3,09E+11	4844
Italy	62007540	2,91E+11	4740
Canada	35362905	5,28E+11	15081
Belgium	11409077	81000000000	7171
Greece	10773253	53000000000	4969
Sweden	9880604	1,27E+11	12983
Austria	8711770	69750000000	8087
Switzerland	8179294	58000000000	7162
Denmark	5593785	32000000000	5778
Finland	5498211	81000000000	14880
		Average	**8265**

According to Eurostat in 2014 in EU, there were on average around 0,45 cars/capita (Eurostat, 2017).

Table 27-Cars per capita according to Eurostat

Country	Cars/capita
Belgium	0,496
Bulgaria	0,416
CzechRepublic	0,448
Germany	0,55
Estonia	0,496
Ireland	0,438
Greece	0,468
Spain	0,471
France	0,483
Croatia	0,347
Italy	0,61
Cyprus	0,558
Latvia	0,329
Lithuania	0,41

Hungary	0,315
Malta	0,625
Netherlands	0,473
Austria	0,552
Poland	0,526
Portugal	0,451
Romania	0,246
Slovenia	0,518
Slovakia	0,36
Finland	0,582
Sweden	0,475
United Kingdom	0,452
Liechtenstein	0,767
Norway	0,5
Switzerland	0,539
Turkey	0,129

As a result, in our power system, there could be 4596750 electric vehicles if we had a 100% penetration of electric vehicles.

3.2.2 Battery capacity and charging

There are two categories of electric vehicles; the plugin hybrids and the fully electric vehicles. In the first category, the battery capacity used varies from 4,4kWh to 17kWh, for example, Toyota Prius III (plug-in hybrid) encapsulates 9kWh and can be charged with a 3,3kW charger, whereas the Chevrolet Volt engages an 18kWh battery and can be charged with a 3,6kW charger. The second category is the fully electric vehicles where someone finds capacities between 19 and 100 kWh (plugincars, 2017).

Table 28-Commercially available electric vehicles and their characteristics

	Battery capacity (kWh)	**Charger(kW)**	**Battery Range(km)**	**Electricity consumption (kWh/km)**
BMW i3	33	7,7	183	0,1799
Chevrolet Bolt	60	7,2	383	0,1566
Chevrolet Spark EV	19	3,3	132	0,1440
Volkswagen E Golf	24	7,2	134	0,1797
Ford Focus Electric	23	6,6	185	0,1243

Nissan Leaf	30	6,6	172	0,1742
TeslaModel S	100	10	507	0,1973

The current research assumes that only fully electric vehicles will be used and thus it is decided to proceed with a 35kWh battery capacity for all the vehicles to be able to complete all the daily journeys on one battery charge.

According to the commercially available models, the consumption of electricity varies between 0,12 to 0,20 kWh/km. We assume 0,175 kWh/km as an average value that represents most of the models of Table 28.

There are different charging options available according to the limits of the power lines. This thesis assumes that a 3kW charger will be used for vehicles running journeys up to 80km and another type of "fast charger" at 6kW maximum charging capacity will be used for vehicles running longer journeys and should be charged before the next morning in a period of 5 to 6 hours.

3.2.3 Driving patterns

The main goal of the model is to reproduce in a realistic way the driving patterns of real life. Therefore, we should process the statistical data from national authorities that are available.

According to the Swedish Institute for Transport and Communication Analysis, which had made an extensive survey of Swedish resident's traveling patterns during the period 1/10/2005 and 30/9/2006, the car is the most common means of transport (TRAFIK ANALYS, 2017).

In that study, the journeys are separated into four broad categories.

1. Business, work, and study -related
2. Service and shopping
3. Leisure
4. Other purpose

For each one of the categories above, it is measured how many journeys start during each hour. To be able to use the statistics we make the following assumptions:

1. The statistics regard journeys with any transport. Therefore, we assume that the same rates apply to car transportation also.
2. The statistics are based on periods of 60 minutes. For convenience reasons, in the model building, we assume that all the journeys start at the end of each period.
3. We assume that trips from categories 1, 2 and 3 are two-way travel, whereas category four journeys are one-way trips.

Table 29-Trips that start withing each hour period categorized by purpose.

Hour	Business, work and study-related	Service and Shopping	Leisure	Other purpose
1	0,09%	0,01%	0,03%	0,01%
2	0,03%	0,00%	0,00%	0,00%
3	0,04%	0,02%	0,01%	0,00%
4	0,05%	0,01%	0,00%	0,00%
5	0,21%	0,01%	0,03%	0,00%
6	1,33%	0,02%	0,08%	0,05%
7	4,63%	0,11%	0,30%	0,06%
8	9,12%	0,44%	0,60%	0,19%
9	4,51%	0,85%	1,08%	0,29%
10	1,62%	1,29%	1,73%	0,35%
11	1,02%	2,27%	2,17%	0,52%
12	1,18%	2,23%	2,30%	0,40%
13	2,08%	1,87%	2,51%	0,36%
14	2,12%	1,68%	2,05%	0,38%
15	3,04%	1,65%	1,95%	0,45%
16	4,27%	1,40%	1,74%	0,39%
17	6,06%	1,36%	2,09%	0,38%
18	2,99%	1,45%	2,79%	0,32%
19	1,26%	0,98%	2,84%	0,32%
20	0,60%	0,59%	1,68%	0,19%
21	0,52%	0,35%	1,15%	0,20%
22	0,64%	0,18%	0,59%	0,08%
23	0,34%	0,08%	0,32%	0,05%
24	0,18%	0,04%	0,18%	0,02%

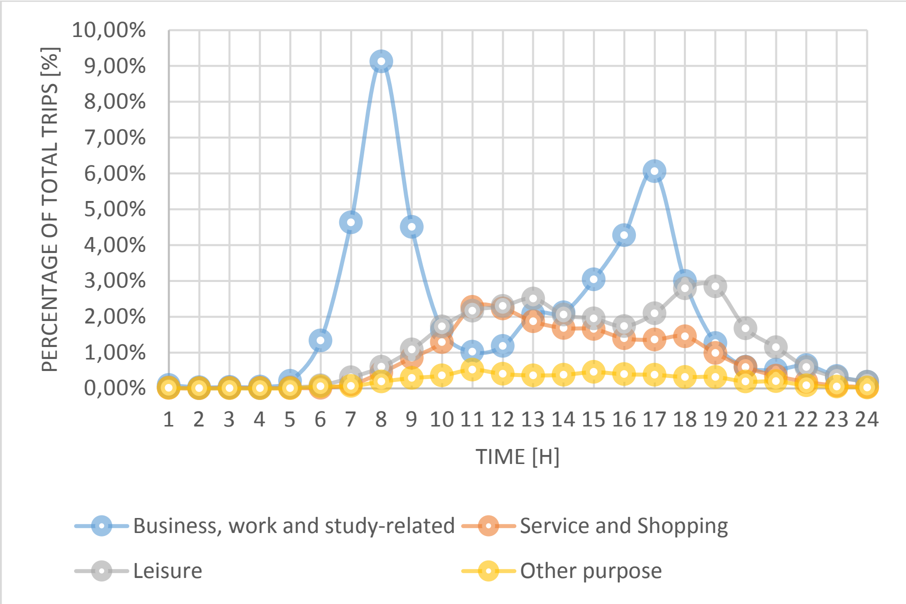

Figure 6-Starting time of different category of trips over a 24-hour period.

The graph above shows that journeys from categories 1, 2 and 3 form two peaks in a way that confirms our assumption that they are two-way trips. The logic behind that is that someone leaves his/her house in the morning and returns later. For example, we observe that work-related journeys peak at 08.00 and then at 17.00 which is a typical schedule for workers. Furthermore, half of the journeys happen until 14.00, and the other half is made after that time, helping us to understand the two-way trips better. For that reason, we aggregate the journeys for the first three categories into one category called two-way journeys and those from the fourth category to one-way trips.

Table 30-Starting time of one-way and two-way trips over a 24 hour period.

Hour	Two-way trips	One way trips
1	0,13%	0,01%
2	0,03%	0,00%
3	0,06%	0,00%
4	0,05%	0,00%
5	0,25%	0,00%
6	1,43%	0,05%
7	5,04%	0,06%
8	10,16%	0,19%
9	6,44%	0,29%
10	4,64%	0,35%
11	5,46%	0,52%

12	5,70%	0,40%
13	6,45%	0,36%
14	5,86%	0,38%
15	6,64%	0,45%
16	7,41%	0,39%
17	9,51%	0,38%
18	7,23%	0,32%
19	5,08%	0,32%
20	2,86%	0,19%
21	2,02%	0,20%
22	1,41%	0,08%
23	0,73%	0,05%
24	0,40%	0,02%

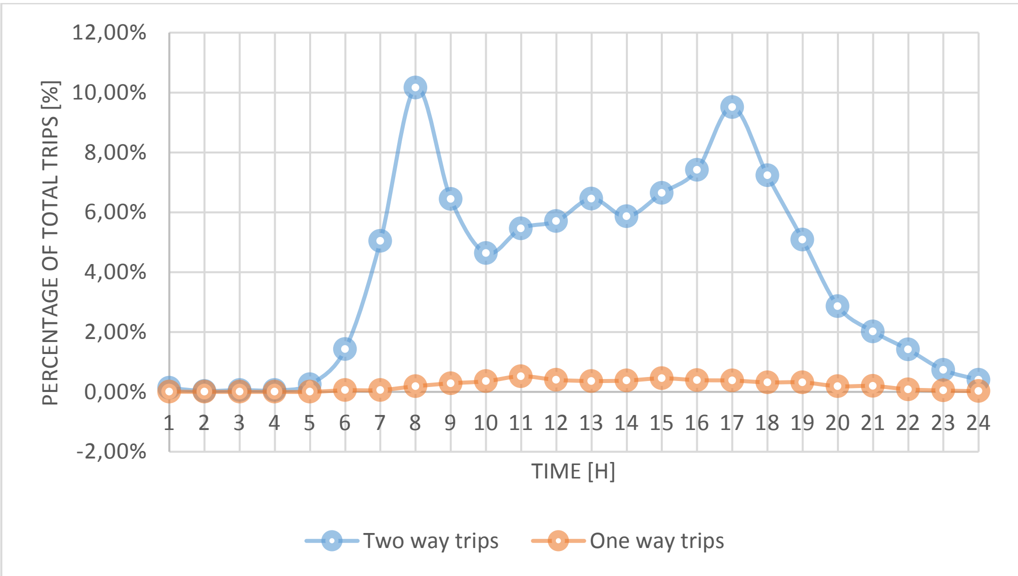

Figure 7 Starting time of one-way and two-way trips over a 24-hour period.

The next graph shows the distribution of trip lengths that will be used for the calculations.

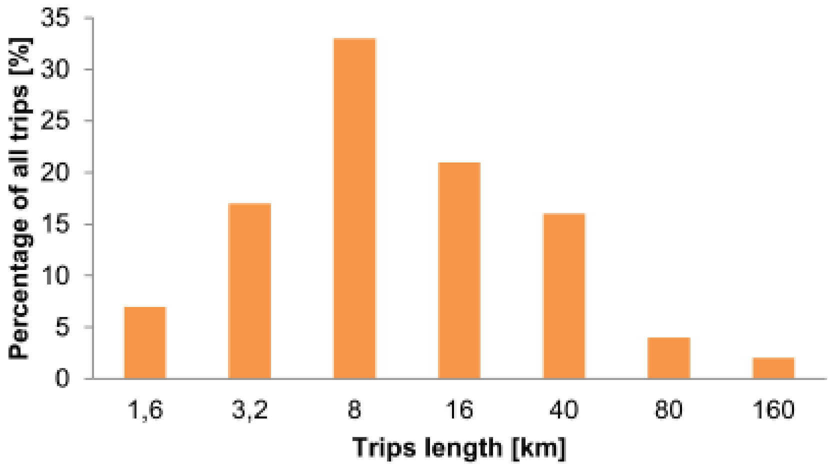

Figure 8-Percentage of trips in each Trip length group (Madzharov, Delarue, & D'haeseleer, 2013).

The average speed used in this research is presented in the following table

Table 31-Average speed for each of the length groups (Andréa & Hammarströmb, 2000).

trip type	trip length [km]	average speed [km/h]
urban roads	1.6	26
urban roads	3.2	26
urban roads	8	26
urban roads	16	26
secondary roads	40	44
main roads	80	86
motorways	160	115

From Table 31, it is derived, that every trip starting in a period will travel for less than an hour and therefore, in an ideal situation it will be charging during the next period. That happens for all the length groups except the longest ones which are the smaller by percentage group.

3.3 Integration of Vehicles Model and Driving patterns into Unit Commitment algorithm

The data gathered in the previous section should now be used in an existing unit commitment algorithm. Thus, using as a base (Madzharov, Delarue, & D'haeseleer, 2013), we develop an algorithm, which will integrate all the electric vehicles data into the unit commitment. We assume that because the data comes from well-developed countries such as the United Kingdom and Sweden should represent a good traveling model for European Union countries and other developed countries.

During night hours (23.00-05.00) we observe a tiny percentage of trips, either one-way or two-way. Thus, we assume that during these hours no trips are taking place and therefore, we distribute these few percentages into the rest time periods. The derived allocation of journeys starting hours is in the following table.

Table 32-Percentage of trips starting during each period over a 24-hour horizon.

H	One-way (%)	Two-way (%)
t1	0,00%	0,00%
t2	0,00%	0,00%
t3	0,00%	0,00%
t4	0,00%	0,00%
t5	0,00%	0,00%
t6	0,01%	1,50%
t7	0,08%	5,10%
t8	0,17%	10,20%
t9	0,25%	6,50%
t10	0,40%	4,70%
t11	0,59%	5,50%
t12	0,40%	5,70%
t13	0,40%	6,40%
t14	0,40%	5,90%
t15	0,50%	6,70%
t16	0,40%	7,40%
t17	0,40%	9,70%
t18	0,25%	7,30%
t19	0,25%	5,10%
t20	0,17%	2,80%
t21	0,17%	2,20%
t22	0,08%	1,50%
t23	0,08%	0,80%
t24	0,00%	0,00%
Sum	**95%**	**5%**

The main purpose of the algorithm is to charge all the vehicles' batteries into a 24 hour horizon day. For example, if a car starts its journey at 6.00 it should be charged by then, but if it starts at 10.00, then it should be charged by 9.00. To this respect, we want in a 24 hours' period to charge the electric consumption of the electric vehicles. The reason why we did not use strict constraints on the charging time is explained by the large number of vehicles that we will use. Consequently, we assume an equal distribution of the 24 hours. Another critical assumption that will be utilized is that due to the size of the electric system, we will equally distribute the number of electric cars on each bus bar and we will further assume that each electric vehicle will always be charged on the same bus bar.

It is important to clarify how the two-way and one-way trips are calculated. A trip in the one-way category is made at once for example at 40km. However, an EV in the two-way category makes two trips at 20km each, therefore in total 40km per day.

The most important number that should be derived from the previous data to perform the desired calculations is the number of EVs that start their journeys each hour.

The total number of EVs in the system, at 100% penetration level, ($EV_{P100\%}$) is the sum of the number of EVs that make one trip (EV_{one}) and the number of EVs that make two trips (EV_{two}) per day:

$$EV_{P100\%} = EV_{one} + EV_{two} \ (26)$$

The number of trips in the one-way group is equal to the number of EVs in that group:

$$Trips_{one} = EV_{one} \ (27)$$

The total number of trips in the two-way group is twice the number of EVs in that group:

$$Trips_{two} = 2 \times EV_{two} \ (28)$$

The total number of trips is equal to the sum of the one-way and two-way group:

$$Trips_{total} = Trips_{one} + Trips_{two} \ (29)$$

In the previous paragraph (Table 32) we calculated that the one-way trips are 5% of the total trips the factor that represents this figure will be from now on called f_1. Then:

$$Trips_{one} = f_1 \times Trips_{total} \ (30)$$

By substituting equations (27) and (28) into equation (29):

$$Trips_{total} = EV_{one} + 2 \times EV_{two} \ (31)$$

By substituting equations (27) and (31) into equation (30):

$$EV_{one} = f_1 \times (EV_{one} + 2 \times EV_{two}) \quad (32)$$

By combining equations (26) and (32), we calculate the number of EVs in the two-way group and then by using that result and equation (26) we extract the number of EVs in the one-way group. Finally, by using these results, we calculate the total trips using only the $EV_{P100\%}$ and f_1.

After $Trips_{total}$ is calculated we use the distributions presented in Figures 7 and 8 to determine the number of EVs starting each hour and how many kilometers each group of EVs runs.

Knowing the number of total trips $Trips_{total}$, the number of trips started each hour and the distance that each group of EVs runs; we can now derive the number of parked EVs in each cluster that is connected to the grid and ready to be charged and their battery capacities *EVsAvailable(e,t)*. Also, the energy that is consumed by the EVs *ConsumedEnergy(e,t)* is calculated. These parameters are now used in the optimization of the unit commitment models.

Chapter 4: Electric Vehicles Load Model and Simulation Results

4.1 Model formulation

In the previously described formulation for the unit commitment model, we will make a few additions to the model to take into account the extra load coming from the EVs that will be charging. The additions that we should make are at two levels: firstly, we should update the excel input file so that the values for the new parameters are introduced to the unit commitment model. Secondly, we should add the new equations and constraints that model the EV load as described before.

In chapter 2 we discussed a unit commitment algorithm and a couple of different implementations. In this paragraph, we will describe the formulation added to that model to integrate a flexible load from EVs.

4.1.1 Nomenclature

A. Indices

e	Index of same distance traveling EVs group1-E

B. Parameters

$Trips_{es}$	Trips started each hour per EV distance group e and bus bar$s$
$EVsAvailable_{es}$	EVs that are available for charging each hour
$Consumption_{e}$	Energy consumption per EVs group e
$BatteryFull_{e}$	Total battery capacity of all cars for each group e
$ChargeLine_{e}$	Power of the charger that each group of EVs can be charged by (MW)
$MaxTransfer_{es}$	Maximum charging load each hour according to the EVsAvailable

C. Variables

$EnergyUp_{es}(t)$	Additional electricity demand for EVs charging in group e in bus s in hour t (MWh)
$soc_{es}(t)$	State of charge of EVs in group e in bus s in period t (MWh)

4.1.2 Equations and Constraints

Firstly, we have to add in the power balance equation the term that represents the EV charging loads. Then the power balance equation is:

$$\sum_{i=1}^{I} g_i(t) - \sum_{\{s,m\}\in L|m>s} B_{sm} \cdot \left(\theta_s(t) - \theta_m(t)\right) - \sum_{\{s,m\}\in L|m<s} B_{ms} \cdot \left(\theta_m(t) - \theta_s(t)\right) = d_s(t) \; \forall \; t \leq T, \quad s \leq S, e \leq E \quad (33)$$

Then, we have to calculate the energy consumption for each bus bar for each EV group for each hour.

$$ConsumedEnergy_{es}(t) = Trips_{es}(t) \cdot Consumption_e \; \forall \; t \leq T, \quad s \leq S, \quad e \leq E \quad (34)$$

Finally, we have to calculate the state of charge for each group of EVs in each bus s in each period t.

$$soc_{es}(t) = soc_{es}(t-1) + n \cdot EnergyUp_{es}(t) - \frac{1}{n} \cdot ConsumedEnergy_{es}(t) \forall \; t \leq T, \quad s \leq S, \quad e \leq E \quad (35)$$

The MaxTransfer parameter is calculated manually outside the model via the equation:

$$MaxTransfer_{es}(t) = EVsAvailable_{es}(t) \cdot ChargeLine_e(t) \; \forall \; t \leq T, \quad s \leq S, \quad e \leq E \quad (36)$$

Finally, we introduce three constraints that ensure that the calculated values will not exceed the appropriate limits.

The first constraint ensures that the charging energy will not be more than the energy needed to top all the batteries.

$$soc_{es}(t-1) + EnergyUp_{es}(t) \leq BatteryFull_{es}\ \forall\ t \leq T, \qquad s \leq S, \qquad e \leq E \quad (37)$$

The following constraint ensures that each hour the charging power will not be more than the maximum output power of the chargers used.

$$EnergyUp_{es}(t) \leq MaxTransfer_{es}(t)\ \forall\ t \leq T, \qquad s \leq S, \qquad e \leq E \quad (38)$$

The last control is that the whole energy that will be used to charge the EVs in each bus bar will be according to the energy that these EVs consumed during the day.

4.2 Input data

In the data input file, we add the following parameters:

Table 33-Trips(t,e,s): The trips that start each hour for each group of EVs (e) for each bus bar (s).

Trips(t,e,s)					
			s101	**s102**	**s103**
t6	**.**	**e1**	130,4002	130,4002	130,4002
t6	**.**	**e2**	304,2671	304,2671	304,2671
t6	**.**	**e3**	588,6119	588,6119	588,6119
t6	**.**	**e4**	376,7116	376,7116	376,7116
t6	**.**	**e5**	291,5893	291,5893	291,5893
t6	**.**	**e6**	72,44454	72,44454	72,44454

Table 34-EvsAvailable(t,e,s): the EVs that are parked and available for charging.

EVsAvailable (t,e,s)					
			s101	**s102**	**s103**
t1	**.**	**e1**	4533,781	4533,781	4533,781
t1	**.**	**e2**	10578,82	10578,82	10578,82
t1	**.**	**e3**	20464,98	20464,98	20464,98
t1	**.**	**e4**	13097,59	13097,59	13097,59
t1	**.**	**e5**	10138,04	10138,04	10138,04
t1	**.**	**e6**	2518,767	2518,767	2518,767

Table 35-Consumption(e): the EVs consumption in MWh according to their distance group.

Consumption(e)	
	column1
e1	0,00028
e2	0,00056
e3	0,0014
e4	0,0028
e5	0,007
e6	0,014
e7	0,028

Table 36-BatteryFull(e): the total capacity of the batteries of EVs in each distance group (e) in (MWh).

BatteryFull(e)	
	column1
e1	11583,81
e2	27028,89
e3	52288,03
e4	33464,34
e5	25902,69
e6	6435,45
e7	4183,043

Table 37-ChargeLine(e): the power of the charger that each group of EVs is mounted on, in MW.

ChargeLine(e)	
	column1
e1	0,003
e2	0,003
e3	0,003
e4	0,003
e5	0,003
e6	0,003
e7	0,006

Table 38-MaxTransfer(t,e,s): the maximum power that could be ejected from the power system for charging the EVs at each hour in MW.

MaxTransfer(t,e,s)					
			s101	**s102**	**s103**
t1	**.**	**e1**	13,60134	13,60134	13,60134
t1	**.**	**e2**	31,73647	31,73647	31,73647
t1	**.**	**e3**	61,39495	61,39495	61,39495
t1	**.**	**e4**	39,29277	39,29277	39,29277
t1	**.**	**e5**	30,41411	30,41411	30,41411
t1	**.**	**e6**	7,556301	7,556301	7,556301

4.3 Simulation properties

4.3.1 Assumptions and simplifications

The previous chapter describes the power system that we used. There are some reasons that we made certain simplifications and assumptions about that power system and the integration of the EVs in it. Firstly, the power system itself is quite big, and a small number of EVs would not affect it in a considerable way. Secondly, we decide that since the number of EVs is big and the driving patterns that we use are based on statistics, the absolute accuracy of our calculations is not within the scope of this research. Furthermore, it would be computationally intensive to model each EV as an only oddity, and it would be computationally impossible to integrate such a large number of EVs in such a big power system in respect to the resources available. That is the reason why we chose the aggregation above method in order to understand the effect from a macro perspective. In that method, the focus is not on every EV that is being charged but on the total additional energy that is needed/required to charge the EVs that are adjusted to each HV bus bar.

4.3.2 Charging Profiles

Our research is based on three charging profiles which were used to evaluate the effects of the extra energy demand in the operation of the electric system.

- Optimized charging profile (Profile 1)

In the optimized charge profile, the charging of the EVs is handled by the unit commitment algorithm which is responsible for distributing the additional energy demand across the 24 hours to achieve the least total economic cost of the operation of the whole system.

- Random charging profile (Profile 2)

In the random charge profile, the charging of the EVs is done after every trip. That means that if an EV is moving during hour 9, then it will start charging right after its trip at hour 10. It can be derived by combining the statistics used for the driving patterns. According to the driving patterns, all the trips in distance groups up to 6 are being completed within an hour from their beginning according to the table (31). According to the table (30) and figure (8) only 2,6% of the trips is 160km and from that only 5 % is made at once which means that only 0,13% of the trips last longer than an hour but also less than two hours. That means that we will consider the same rule for all the EVs which mean that if a trip starts at hour 9 then its charge will start at hour 10. This profile will test if the energy production capacity of the system is adequate to charge a large number of EVs during the peak hours.

- Off-peak charging profile (Profile 3)

In the off-peak-charge profile, all the EVs can charge only during the off-peak hours which means that the charging is done during hours 1-8 and 21-24. This charging profile was selected to verify the operation of the unit commitment algorithm and our global assumption that the power system operates better when we do not have big ramps in power demand.

4.3.3 Selection of unit commitment models

The unit commitment models used to evaluate the effect of the extra load demand from EVs are the deterministic, the stochastic and the interval unit. The decision intending to testing the effect of the excess load on unit commitment models of different robustness.

The deterministic model is the easiest to be solved and provides a solution which is based on a static prediction of the wind power generation. However, that prediction relies on some statistics and data processing on historical data.

The stochastic model is using ten different scenarios of the wind power production forecast. Each scenario is paired with a probability to happen according to its likelihood to occur. However, it is not within the scope of this research to analyze the mathematical methods used to generate the most typical scenarios from the historical data.

The interval unit model is much more conservative than the other two because it commits units to meet the extreme transitions which are extracted from the wind data.

4.4 Results

4.4.1 Deterministic model results

We ran the deterministic model for the three charging scenarios, and we present the effect on the electricity demand in the following figures.

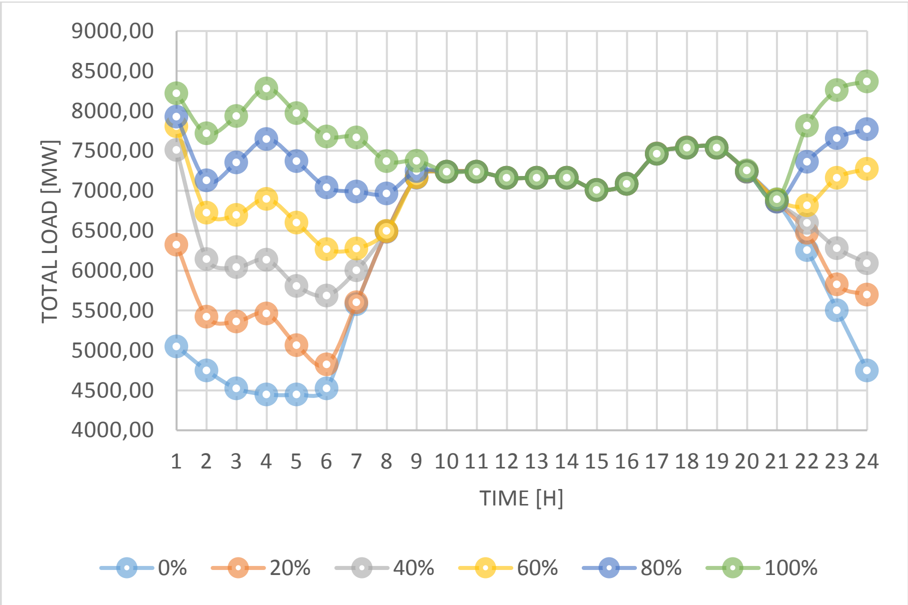

Figure 9-Total load for Deterministic model solution under optimized charging profile for different electric vehicles penetration

The first and most important result is that the optimized charging profile chooses to allocate the extra electricity demand during the hours that the average demand is low. This action leads to keep the units that would normally be closed, committed to keep up with the standard demand during peak hours. The avoidance of the startup costs will lead to higher efficiency and better use of non-flexible units such as the coal-fired units.

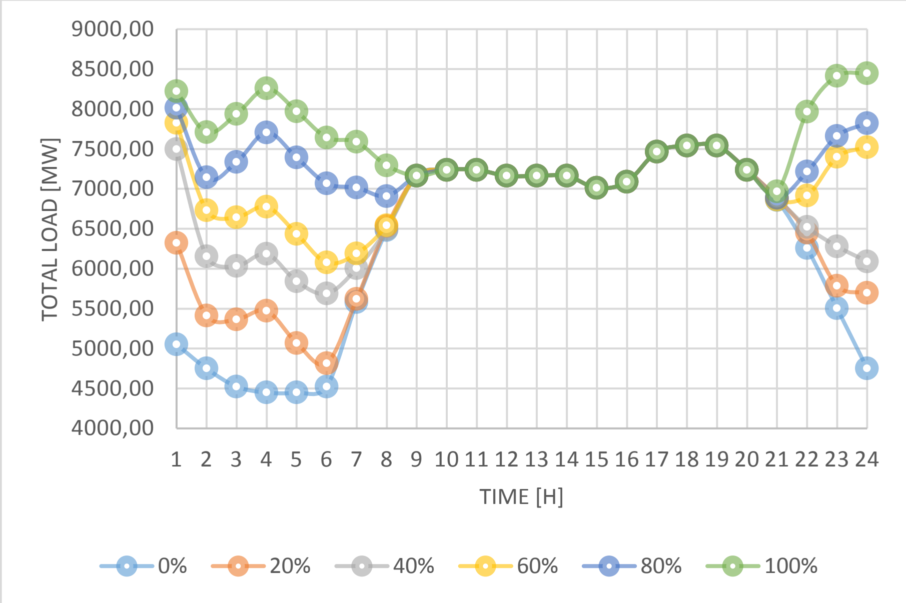

Figure 10-Total load for Deterministic model solution under off-peak charging profile for different electric vehicles penetration.

The second observation we make is that as initially assumed the optimized charging profile has similar results with the off-peak hours charging profile and this is why we expect to have similar total operational costs between those two charging profiles. This result is confirmed by the total operational cost curves of the following figure.

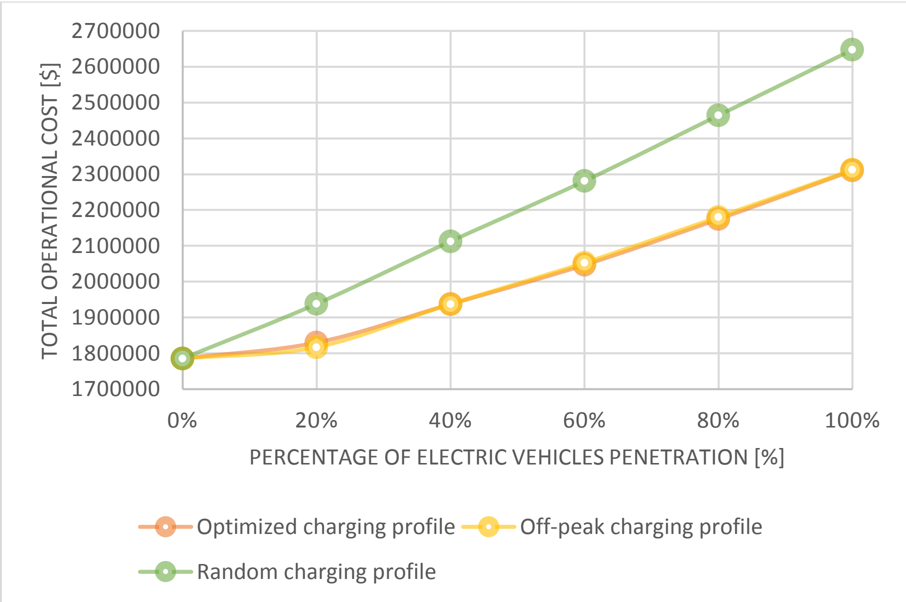

Figure 11-Total operational cost ($) of the Deterministic model under different charging profiles for various electric vehicles penetration.

Finally, in the figure of the random charging profile, we can test the adequacy of thermal power production.

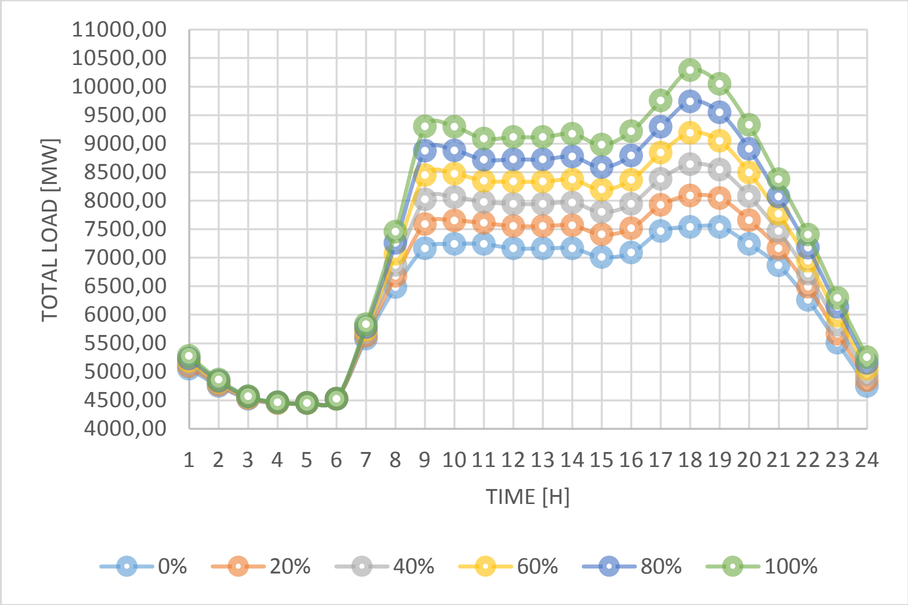

Figure 12-Total load for the Deterministic model solution under random charging profile for different electric vehicles penetration.

If we take the worst case that is when we have 100% penetration of EVs we can compare the maximum load against the maximum total capacity that is available. In this comparison, it is important to take into account the renewable energy production as this is a considerable amount of 30% of the total daily energy production. To test the system in challenging situations, we selected a non-favorable wind profile which gives us much power when the load is low, and the production is low when the demand is very high.

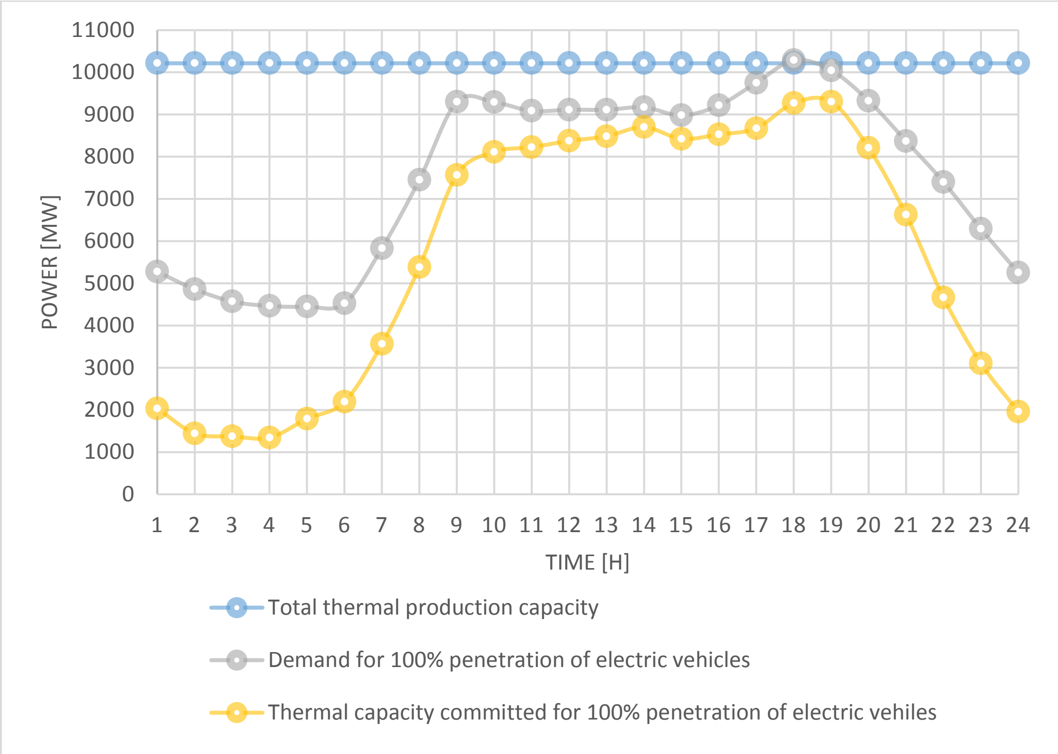

Figure 13-Overview of maximum load for 100% electric vehicles penetration under random charging profile and maximum production capacity.

In that Figure, the blue line shows the maximum thermal production capacity of the power grid. The gray line represents the total load when there is a maximum penetration of electric vehicles. That figure shows that for time interval 18 the load cannot be covered only by the thermal production, but the wind production can fill in the gap. The same hour we can see that the committed capacity is below the maximum available, but we should also consider that some units might be unavailable for production due to problems or regular maintenance schedules. That leads to the conclusion that if we do not use any smart charging scheduling techniques, it is possible to need to build additional thermal power plants to meet peak hours' demand in the future.

In power systems with high renewable energy production penetration is vital to absorb as much renewable energy as possible, to enhance the operation of such units and take the full potential of low carbon emitting units. The results of the wind curtailment in our power system show that flexible load from EVs can be beneficial for the operation of renewable sources and the environment when combined with smart-charging mechanisms or market signals to EVs holders or users.

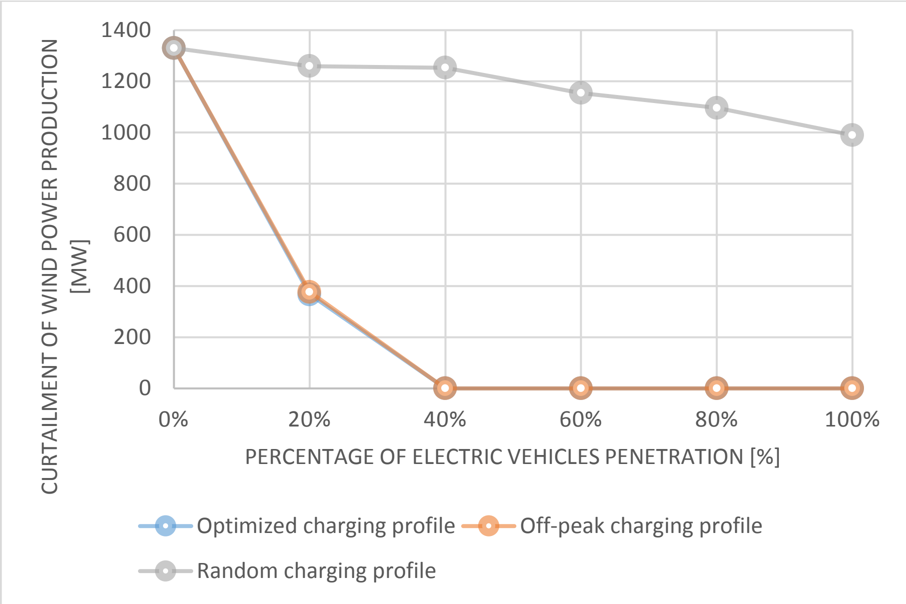

Figure 14-Wind power production curtailment of the Deterministic model under different charging profiles for various electric vehicles penetration.

Finally, it is important to investigate the percentage of increase in the total cost per MWh in respect with the of EVs penetration rate. The following figure helps us draw some conclusions about that.

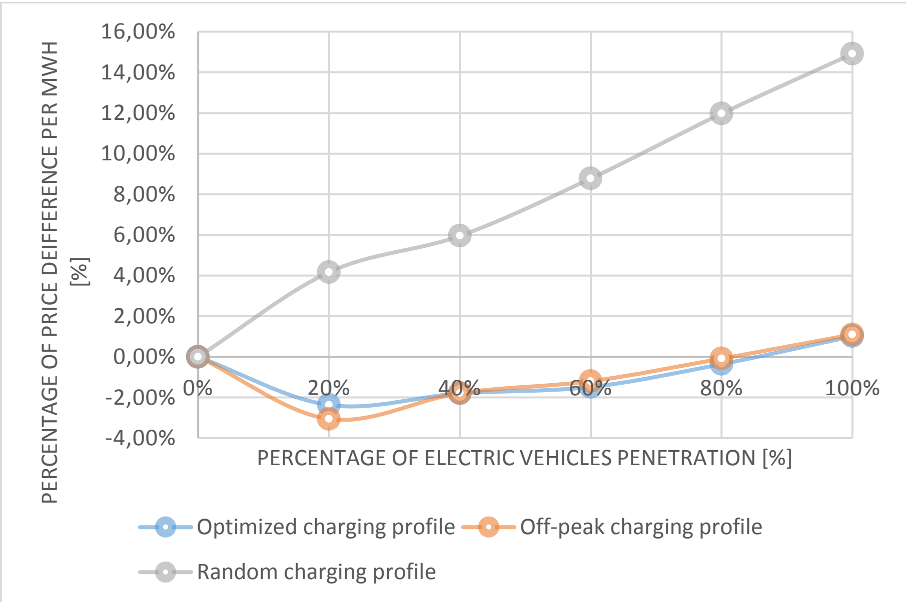

Figure 15-Percentage difference of energy cost ($/MWh) of the Deterministic model solution based on 0% electric vehicles penetration energy cost.

Firstly, we can see that the increase when using the optimized charging profile does not exceed 1,1% in 100% EVs penetration. Secondly, in the random charging profile, we have a much higher increase which is growing faster after 40% of EVs penetration. That could be explained because after this certain percentage it will be mandatory to commit the most expensive units available. We also observe that there is a slight decrease of the price in the optimized charging profile and the off-peak hours charging profile. That has to do with the wind profile and the units committed. As we said before, we have used a non-favorable wind profile with high production during off-peak hours and low production during peak load hours. That leads to shutting down many inflexible units during the off-peak hours and starting them up to meet peak loads. When we add the flexible load, it is distributed across those off-peak hours in a way that the system does not need to shut down those expensive to start units. That is the reason why the cost decreases at first.

4.4.2 Stochastic model results

We ran the stochastic model for the same three charging scenarios, and we present the effect on the electricity demand in the following figures. The procedure to extract the data is the following: as long as we have ten different unit commitment results, we multiply each result with the probability of the scenario. Afterward, all the weighted results are summarized to the final result.

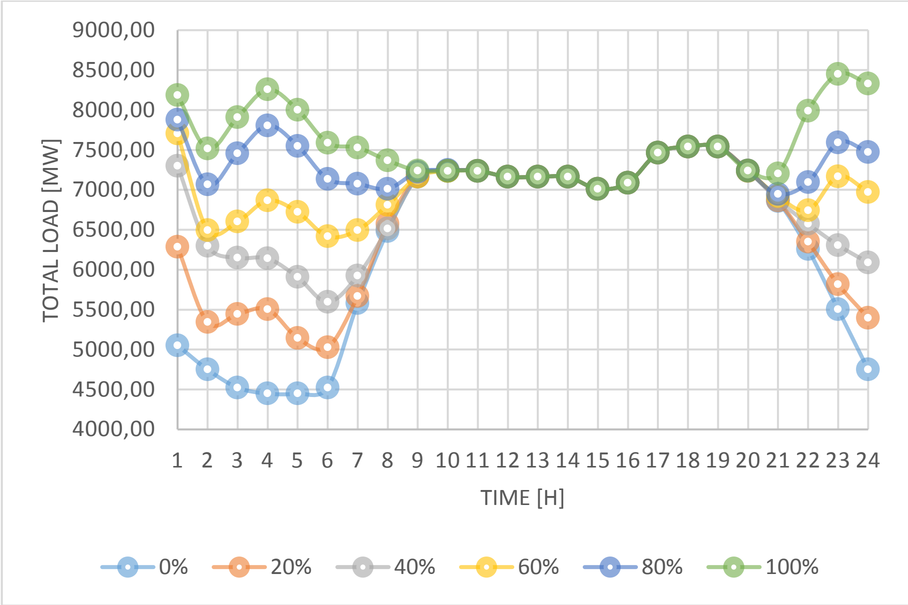

Figure 16-Total load for the Stochastic model solution under optimized charging profile for various electric vehicles penetration.

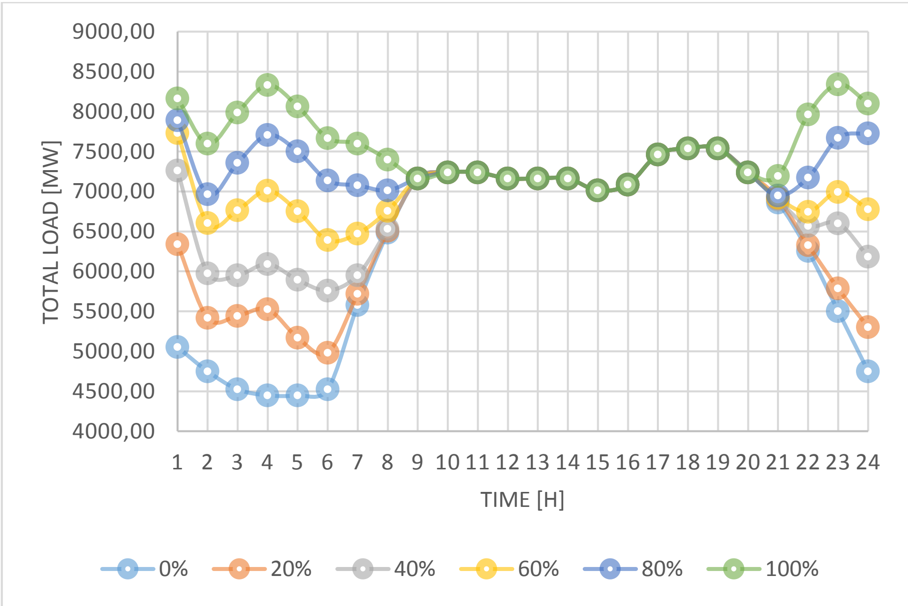

Figure 17-Total load for the Stochastic model solution under off-peak charging profile for various electric vehicles penetration.

Similarly, to the deterministic model the results of the committed capacity when using charging profile 1 and 3 have minor differences. This conclusion comes out both from the load demand charts and the total thermal production cost chart.

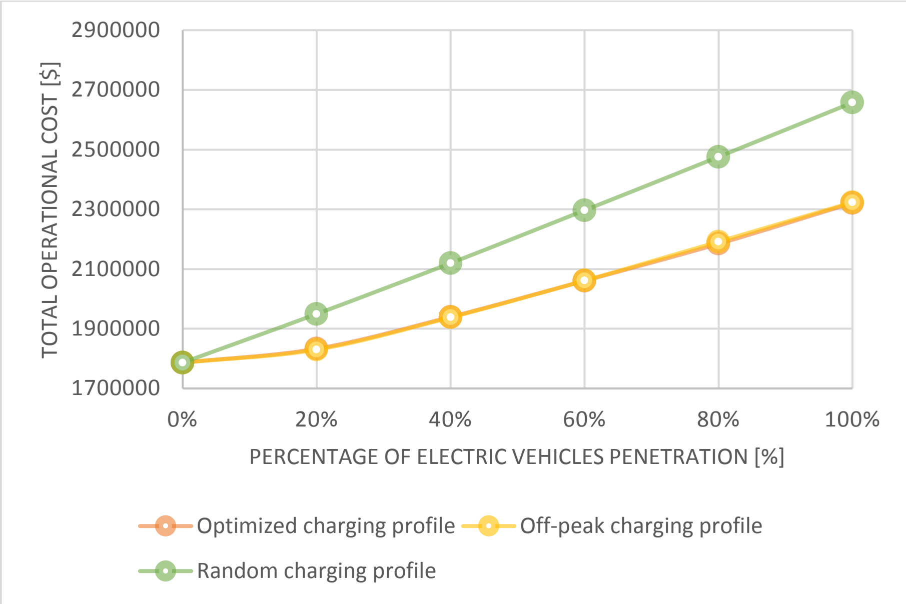

Figure 18-Total operational cost ($) of the Stochastic model under different charging profiles for various electric vehicles penetration.

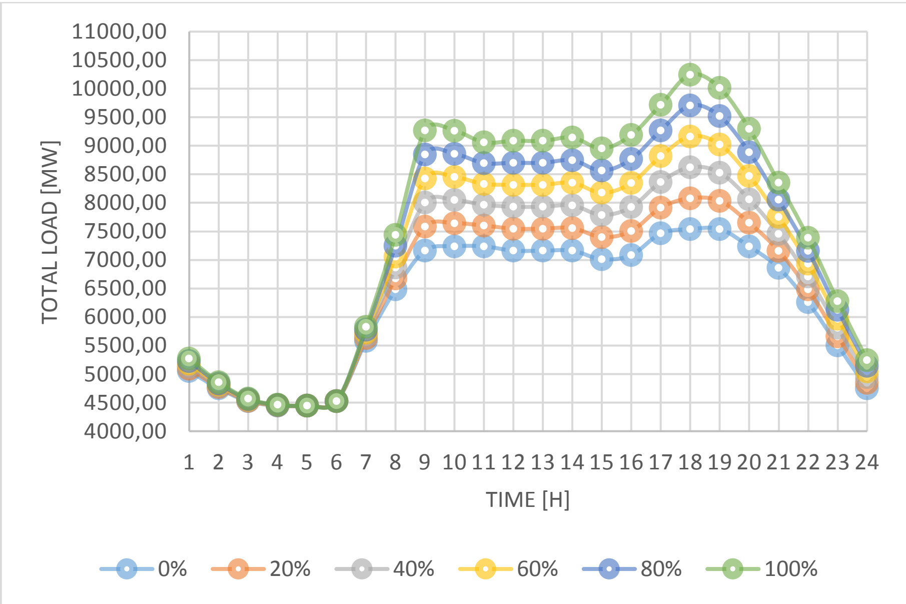

Figure 19-Total load for the Stochastic model solution under random charging profile for various electric vehicles penetration.

When using charging profile two, we can see from the diagram that the maximum load in 100% EVs penetration exceed the total thermal production capacity slightly during hour 18 of the planning horizon. Wind power capacity helps the system to meet the load demand although there should be an emergency plan in case of unexpected outages in production units. For the stochastic model, we have the same conclusion as for the deterministic model.

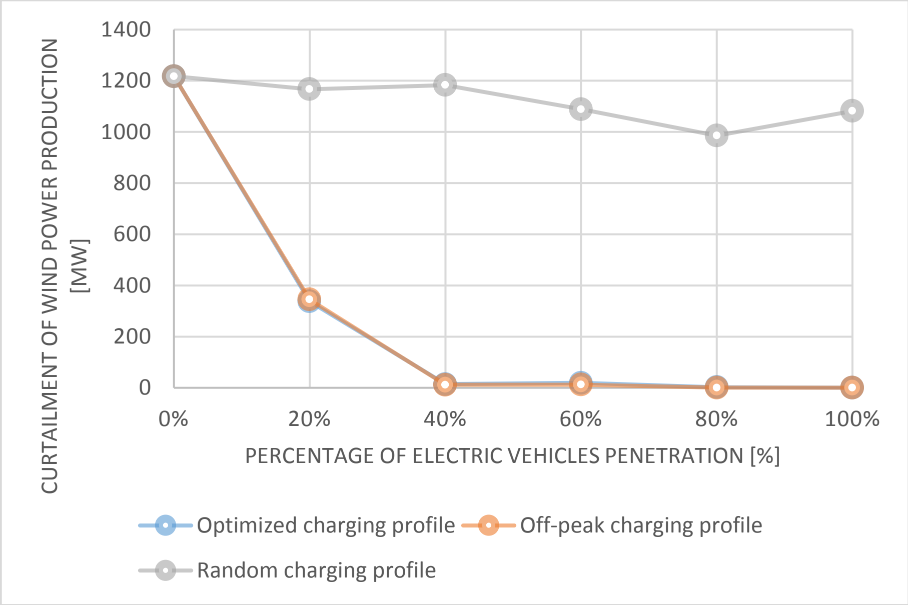

Figure 20-Wind power production curtailment of the Stochastic model under different charging profiles for various electric vehicles penetration.

The wind production curtailment curves show us that the additional load from EVs can absorb some or all of the curtailed production especially when it is combined with an efficient charging method. However even when using the random charging profile, there is a slight decrease in the curtailed production. In any case, the curtailed production is a small percentage of the total demand, and we cannot make final conclusions, but there is an indication that excessive renewable energy can charge extra load from electric vehicles.

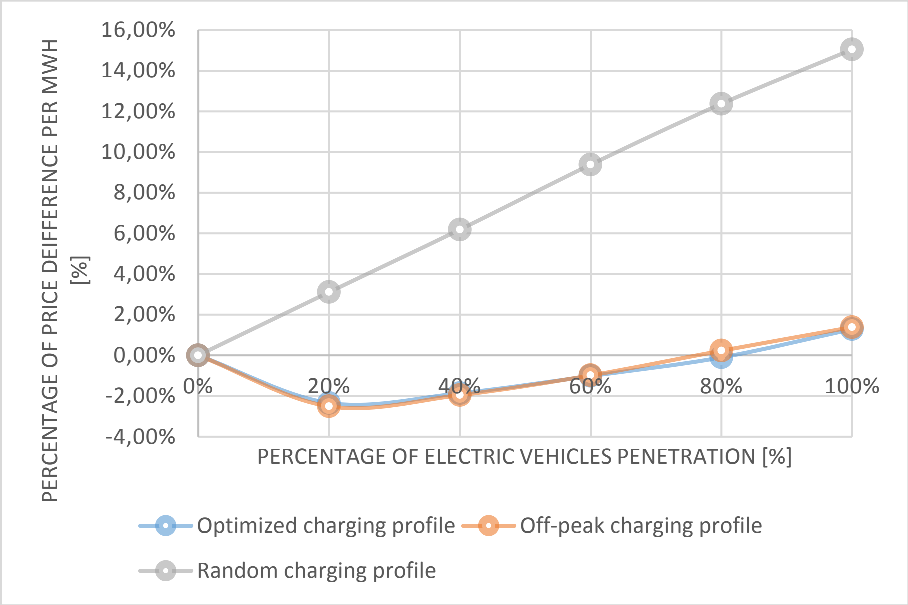

Figure 21-Percentage difference of energy cost ($/MWh) of the Stochastic model solution based on 0% electric vehicles penetration energy cost.

The form of the curves for each charging profile for different EVs penetration is similar to those for the deterministic model. As the number of EVs is increasing from 0% to nearly 80%, we observe that the cost for each MWh of energy produced is lower than in 0%. The explanation is that many expensive coal-fired units are used more efficiently while there is no need to shut them down during the low load hours and start them up again later when the load is higher. The avoidance of such startup and shut down costs is vital for the total production cost. However, we observe that in 100% penetration of EVs the percentage of increase of the cost is slightly higher than in the deterministic model for all the charging profiles.

The conclusion from the above is that the model has a similar operation to the deterministic approach with a slightly higher operational cost, caused by the introduction of the stochastic nature of wind production.

4.4.3 Interval unit model results

We ran the interval unit model for the same three charging scenarios, and we present the results in the following Figures.

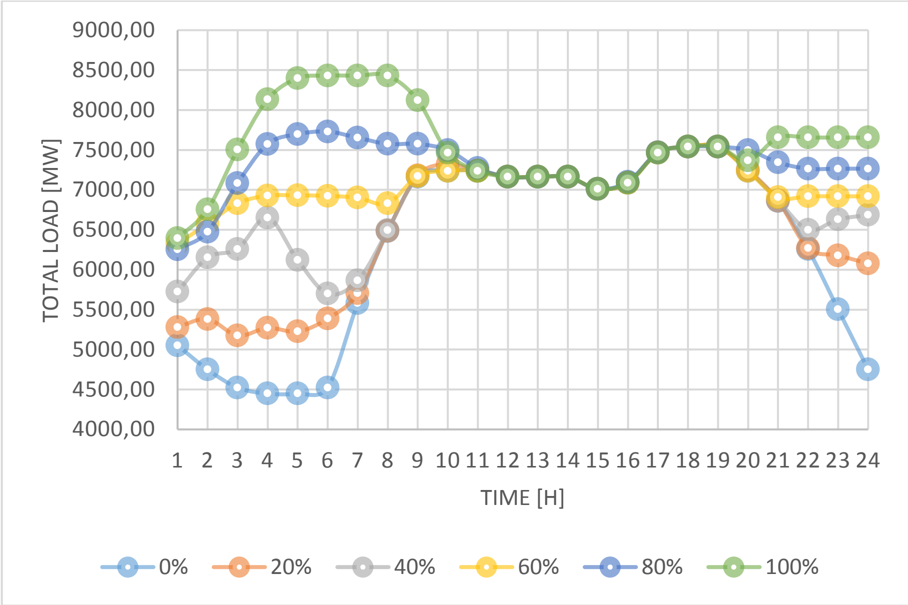

Figure 22-Total load for the Interval model solution under optimized charging profile for various electric vehicles penetration.

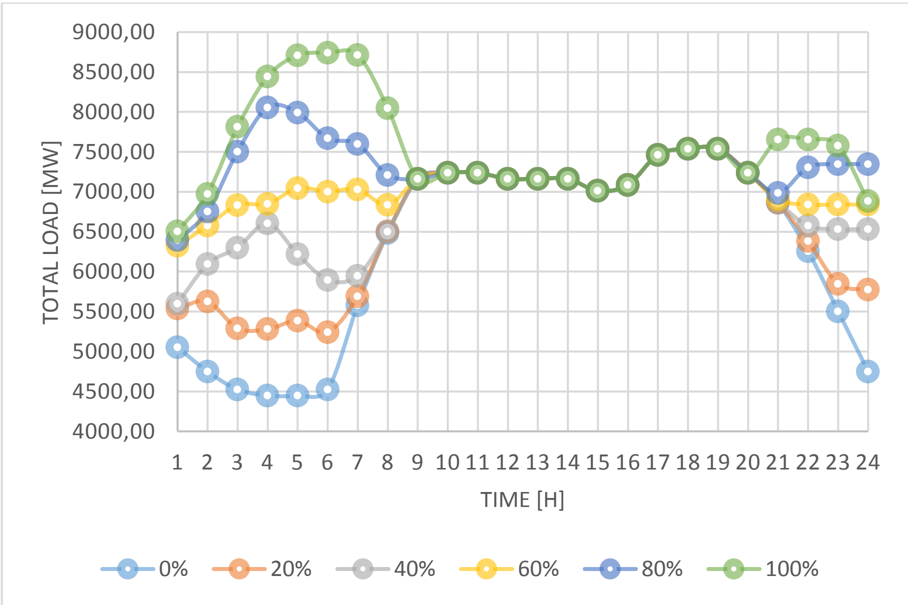

Figure 23-Total load for the Interval model solution under off-peak charging profile for various electric vehicles penetration.

First of all, we observe that the form of the load curves is different from the other two models. In this case, due to the higher robustness the algorithm distributes in a different way the flexible load than in the previous models. On the other hand, we observe that the curves when using charging profile 1 and 3 are very similar, as in the previous models.

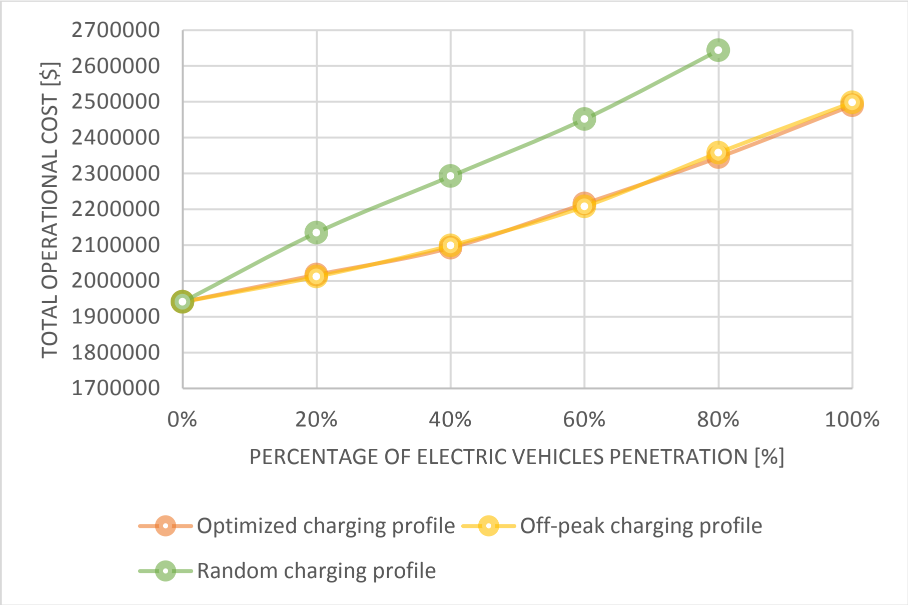

Figure 24-Total operational cost ($) of the Interval model solution under different charging profiles for various electric vehicles penetration.

The curves of the total operational cost have the same form as in the previous models. Specifically, the charging profile 1 and 3 have a similar cost, and profile 2 has a higher cost. However, the level of the total cost is significantly greater than in the previous models.

We have to mention that when using the random charging profile two it is not possible to run the simulation in full (100%) EVs penetration because the total production capacity is not enough to meet the demand. That is a major difference from the previous models. As we can see the system when using a higher robustness unit commitment algorithm, the installed power plants are not able to provide enough electricity for the maximum number of EVs.

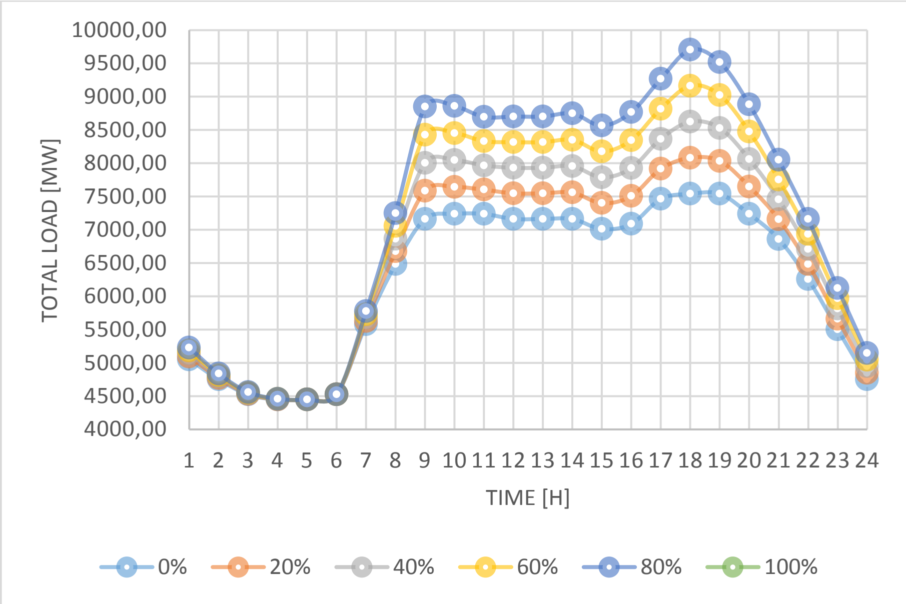

Figure 25-Total load for the Interval model solution under random charging profile for various electric vehicles penetration.

The figure with system load demand in charging profile 2 is similar to the previous model while the profile and the load are the same. However, the 100% EVs penetration curve is missing for the reasons explained beforehand.

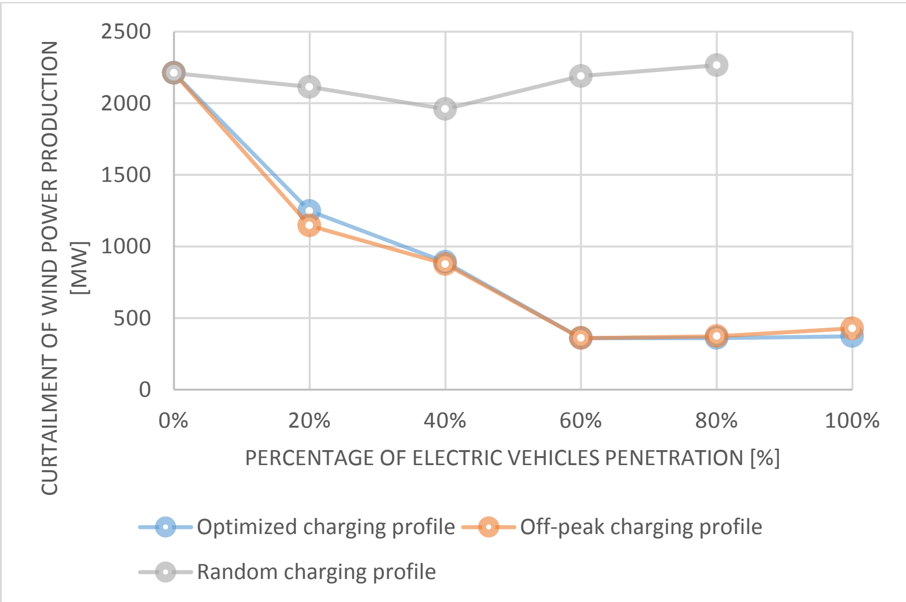

Figure 26-Wind power production curtailment of the Interval model under different charging profiles for various electric vehicles penetration.

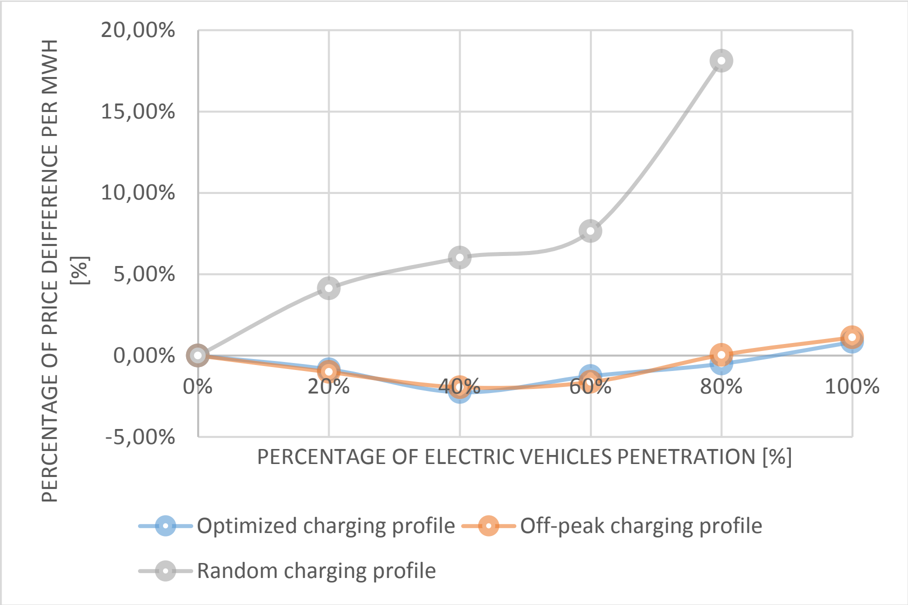

Figure 27-Percentage difference of energy cost ($/MWh) of the Interval model solution based on 0% electric vehicles penetration energy cost.

The curve for the random charging profile energy cost difference is smooth at the beginning until 60% of electric vehicles penetration, and then it is very steep. That phenomenon can be explained by the higher unit capacity commitment of the interval model. As mentioned in Chapter 2 the interval model commits more units to be able to cover extreme transitions of the wind power production as a result of low additional load the capacity is already committed. However, for higher additional loads, it commits the most expensive units.

The results of this model are quite different from the previous models. First of all, the available thermal production capacity was not enough to run the random charge profile for 100% of EVs penetration. Secondly, we have a higher total operational cost in all cases due to higher reliability of the method. Thirdly, we have much more wind energy production curtailed which comes from the increased reliability of the solution produced.

4.5 Models Comparison

Finally, we are presenting a comparison between the three models regarding total operational cost, which reflects the total committed unit's capacity. The results for the deterministic model is the base on which we are calculating the percentage differences between the deterministic and each of the other two models (stochastic and interval).

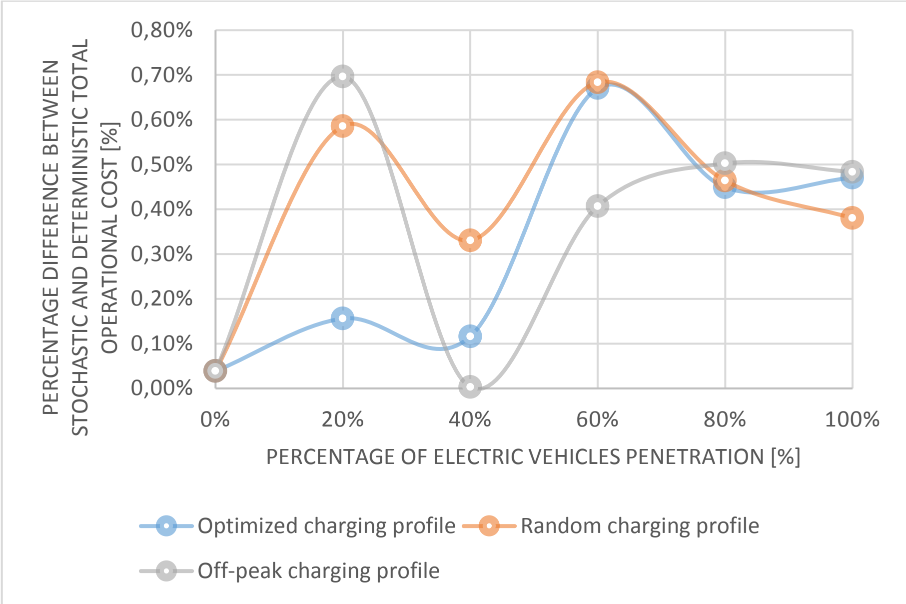

Figure 28-Comparison between the Stochastic model and the Deterministic model total operational cost.

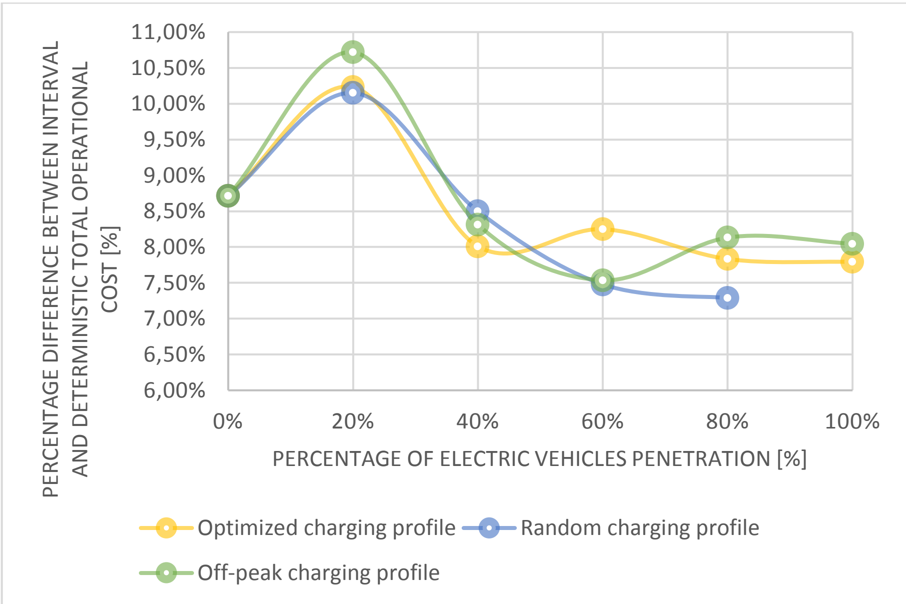

Figure 29-Comparison between the Interval model and the Deterministic model total operational cost.

The comparison shows that the deterministic model is the cheapest one as it commits the capacity needed for the most probable (deterministic) scenario. The stochastic scenario is slightly more expensive than the deterministic as it introduces ten scenarios of wind production. Finally, the Interval model is the most expensive, taking into account that it is the most robust compared to the others.

From figures 9 and 16 we derive that Deterministic and Stochastic model allocate the EVs load in a similar way whereas the Interval model allocates it in a different way. That can be explained by the fact that interval model handles the uncertainty of the wind production differently. The similarity of the Stochastic and Deterministic model is coming from the procedure used to create the deterministic scenario of wind production. The data that were used are the same, and the scenarios were extracted by using certain scenarios reduction methods. As a result, when combining the ten most probable scenarios into one then the outcome should be very close to the one most likely scenario (deterministic).

Chapter 5: Summary and Conclusions

5.1 Conclusion discussion

This thesis presents five mixed-integer linear programming unit commitment models which incorporate high levels of renewable energy production. Each of these models uses different methods to integrate the uncertainty from the renewables. Three of those models were chosen for the integration of electric vehicles load. Our focus is on the effects of the excessive load on the production side, hence cost of production and power grid adequacy to handle the extra load under different charging strategies. The models that were used are the Deterministic, the Stochastic and the Interval. Finally, a comparison between the various models is made.

The selected power system is IEEE RTS 96, and the penetration levels of electric vehicles vary from 0% to 100% with 20% steps. For the simulations were used two charging strategies and the third one for confirmation. The first charging profile is a centrally controlled optimized profile, in which the unit commitment algorithm selects the hours that will be allocating the excess load, to minimize the total production cost. The second charging profile is used to stress the power system and check the penetration levels of electric vehicles that the system is ready to incorporate. The charging under the second strategy is done right after each vehicle's trip and until is fully charged. The third charging strategy was an off-peak hour charging profile, in which the electric vehicles could be charged only during hours 1-8 and 21-24.

Simulation results show that an optimized charging strategy is much more efficient than the random charging strategy. The average cost of energy for the optimized charging for 100% of electric vehicles penetration is not increasing more than 1,5% compared to the cost of energy for 0% electric vehicles penetration. On the other hand, for the random charging strategy, the equivalent cost increases up to 15% for the same conditions. Furthermore, the advantage of using an optimized charging is the ability to integrate more electric vehicles, which was shown when used the more robust unit commitment model (Interval). In that case, the model was not able to run for the 100% penetration due to lack of production capacity. Finally, the third charging profile gave us similar results with the optimized charging profile.

The comparison between the models confirmed our theoretical assumptions. The results show, that the most robust model (Interval) gives an average 8,5% more expensive solution than the less robust model. However, the middle robustness model (Stochastic) solution is only 0,36% more expensive than the solution of the Deterministic model.

5.2 Future Work

Future work on this topic should include the integration of more types of renewable sources, such as photovoltaics and biomass to have a more realistic power system. Furthermore, a higher number of electric vehicles might be used, to investigate the limits of the power system and quantify the scale of investments that might be needed in certain cases, to maintain the ability of the system to handle the load demand. Thirdly, there could be improvements on the model of electric vehicles by further studying of the technologies used, as well as the usage of Vehicle-to-Grid technologies. Additionally, there could be further improvements on the driving patterns. The patterns that were used are the same for the whole system. However such a big system might include different type of cities and villages, where people certainly have different driving patterns. Finally, it is possible to calculate the avoidance of CO2 emissions both from the production side due to massive renewable energy sources penetration and the transportation sector due to the replacement of the internal combustion engines vehicles by the fully electric ones.

References

(2017, 3 28). Retrieved from Eurostat: http://ec.europa.eu/eurostat/tgm/table.do?tab=table&init=1&plugin=1&language=en&pcode=tsdpc340

(2017, 03 29). Retrieved from plugincars: http://www.plugincars.com/cars

(2017, 2 23). Retrieved from TRAFIK ANALYS: http://www.trafa.se/globalassets/sika/sika-statistik/ss_2007_19_eng.pdf

(2017, 2 24). Retrieved from The National Archives: http://webarchive.nationalarchives.gov.uk/+/http:/www.dft.gov.uk/pgr/sustainable/carbonreduction/low-carbon.pdf

(2017, 05 06). Retrieved from European Environment Agency: https://www.eea.europa.eu/publications/towards-a-green-economy-in-europe

Andréa, M., & Hammarströmb, U. (2000). Driving speeds in Europe for pollutant emissions estimation. *Transportation Research Part D: Transport and Environment*, 321-335.

Bertsimas, D., Litvinov, E., Sun, X. A., Zhao, J., & Zheng, T. (2013). Adaptive Robust Optimization for the Security Constrained Unit Commitment Problem. *IEEE Transactions on Power Systems, 28*(1), 52-63.

Boumis, T. (2012). *Energy management of electric vehicles, developing a game theory model, in order to provide ancillary services to grid.* Athens: National Technical University of Athens.

C6.20, C. W. (2015). *Integration of Electric Vehicles in Electric Power Systems.* CIGRE.

Capros, P., Vita, A. D., Tasios, N., Papadopoulos, D., Siskos, P., Apostolaki, E., . . . Witzke, H. P. (2013). *EU ENERGY, TRANSPORT AND GHG EMISSIONS TRENDS TO 2050.* Luxemburg: EUROPEAN COMMISSION, Directorate-General for Energy, Directorate-General for Climate Action and Directorate-General for Mobility and Transport.

Clement-Nyns, K., Haesen, E., & Driesen, J. (2009). The Impact of Charging Plug-In Hybrid Electric Vehicles on a Residential Distribution Grid. *IEEE Transactions on Power Systems*, 371-380.

Dvorkin, Y., Pandžić, H., Ortega-Vazquez, M. A., & Kirschen, D. S. (2015). A Hybrid Stochastic/Interval Approach to Transmission-Constrained Unit Commitment. *IEEE Transactions on Power Systems, 30*(2), 621 - 631.

Europe 2020 in a nutshell. (2017, 04 20). Retrieved from European Commission: Prospective study on the impact of electrical vehicles on the winter load peak in a village of East of

European Commission. (2017, 05 4). Retrieved from https://ec.europa.eu/commission/priorities/energy-union-and-climate_en

European, Parliament, & Counsil. (2009). Directive 2009/33/EC of the European Parliament and of the council of 23 April 2009 on the promotion of clean and energy-efficient road transport vehicles. *Official Journal of the European Union*, 5-11.

GRAHN, P. (2013). *Electric Vehicle Charging Impact on Load Profile.* Stockholm: Royal Institute of Technology.

Kasten, P., Bracker, J., Haller, M., & Purwanto, J. (2016). *Electric mobility in Europe – Future impact on the emissions and the energy systems.* Berlin: Öko-Institut e.V.

Kirschen, D. (2017, 3 15). Retrieved from GridOPTICS: http://gridoptics.org/fpgws14/files/workshop/Kirschen-SCUCVariantsSoftwareSession_GOWS_FY14.pdf

Kirschen, D., Pandzic, H., Dvorkin, Y., Wang, Y., & Qiu, T. (2017, 4 28). Retrieved from Federal Energy Regulatory Commission: https://www.ferc.gov/CalendarFiles/20140624083129-T1A%20-%202%20-%20Kirschen%20Unit%20Commitment.pdf

Madzharov, D., Delarue, E., & D'haeseleer, W. (2013). Integrating electric vehicles as flexible load in unit commitment. *Energy, 65*, 285-294.

Pandzic, H., Dvorkin, Y., Wang, Y., Qiu, T., & Kirschen, D. (2016). Toward cost-efficient and reliable unit commitment under uncertainty. *Power and Energy Society General Meeting* (pp. 970-982). Boston, MA, USA: IEEE.

Pandžić, H., Qiu, T., & Kirschen, D. S. (2013). Comparison of state-of-the-art transmission constrained unit commitment formulations. *2013 IEEE Power & Energy Society General Meeting* (pp. 1-5). Vancouver, BC, Canada: IEEE.

Renewable Energy Analysis Lab - Library. (2017, 4 15). Retrieved from Renewable Energy Analysis Lab: http://www2.ee.washington.edu/research/real/index.html

Schill, W.-P., & Gerbaulet, C. (2015). Power System Impacts of Electric Vehicles in Germany: Charging with Coal or Renewables? *Discussion Papers of DIW Berlin*.

Simoglou, C. K., Biskas, P. N., & Bakirtzis, A. G. (2010). Optimal Self-Scheduling of a Thermal Producer in Short-Term Electricity Markets by MILP. *IEEE Transactions on Power Systems*, 1965-1977.

The World Factbook. (2017, 3 16). Retrieved from Central Intelligence Agency: https://www.cia.gov/library/publications/resources/the-world-factbook

Tomic, J., & Kempton, W. (2007). Using fleets of electric-drive vehicles for grid support. *Journal of Power Sources*, 459-468.

Willett, K., & Jasna, T. (2005). Vehicle-to-grid power implementation: From stabilizing the grid to supporting large-scale renewable energy. *Journal of Power Sources*, 280-294.